

AD-A084 254

UNIVERSAL ENERGY SYSTEMS INC DAYTON OHIO

F/G 11/1

ELECTRON SPECTROSCOPIC STUDIES OF SURFACES AND INTERFACES FOR A--ETC(U)

JAN 80 G E HAMMER, J T GRANT

F33615-77-C-5040

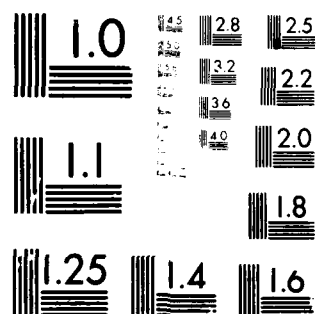
UNCLASSIFIED

AFML-TR-79-4220

NL

1 OF 1
AD
20142714

END
DATE
FILMED
6-80
DTIC



MICROCOPY RESOLUTION TEST CHART
NATIONAL BUREAU OF STANDARDS-1963-A

ADA 084254

AFML-TR-79-4220

LEVEL *AD57984*

2

DTIC
ELECTE
MAY 9 1980
S **D** **C**

**ELECTRON SPECTROSCOPIC STUDIES OF
SURFACES AND INTERFACES FOR
ADHESIVE BONDING**

GERALD E. HAMMER

J. T. GRANT

*UNIVERSAL ENERGY SYSTEMS, INC.
3195 PLAINFIELD ROAD
DAYTON, OHIO 45432*

JANUARY 1980

TECHNICAL REPORT AFML-TR-79-4220
Final Report for period January 1977 — August 1979

Approved for public release; distribution unlimited.

DWG FILE COPY

**AIR FORCE MATERIALS LABORATORY
AIR FORCE WRIGHT AERONAUTICAL LABORATORIES
AIR FORCE SYSTEMS COMMAND
WRIGHT-PATTERSON AIR FORCE BASE, OHIO 45433**


80 5-05-050

NOTICE

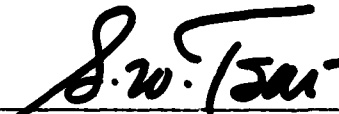
When Government drawings, specifications, or other data are used for any purpose other than in connection with a definitely related Government procurement operation, the United States Government thereby incurs no responsibility nor any obligation whatsoever, and the fact that the Government may have formulated, furnished, or in any way supplied the said drawings, specifications, or other data, is not to be regarded by implication or otherwise as in any manner licensing the holder or any other person or corporations, or conveying any rights or permission to manufacture, use, or sell any patented invention that may in any way be related thereto.

This report has been reviewed by the Information Office (OI) and is releasable to the National Technical Information Service (NTIS). At NTIS, it will be available to the general public, including foreign nations.

This technical report has been reviewed and is approved for publication.




T. W. HAAS, Project Engineer
Mechanics & Surface Interactions Br.
Nonmetallic Materials Division



S. W. TSAI, Chief
Mechanics & Surface Interactions Br.
Nonmetallic Materials Division

FOR THE COMMANDER



F. D. CHERRY
Acting Chief
Nonmetallic Materials Division

"If your address has changed, if you wish to be removed from our mailing list, or if the addressee is no longer employed by your organization, please notify AFWAL/MLBM, W-PAFB, Ohio 45433 to help us maintain a current mailing list".

Copies of this report should not be returned unless return is required by security considerations, contractual obligations, or notice on a specific document.

SECURITY CLASSIFICATION OF THIS PAGE (When Data Entered)

19. REPORT DOCUMENTATION PAGE		READ INSTRUCTIONS BEFORE COMPLETING FORM	
1. REPORT NUMBER	2. GOVT ACCESSION NO.	3. RECIPIENT'S CATALOG NUMBER	
18 AFML TR-79-4220	AD-408425	9	
4. TITLE (and Subtitle)	5. TYPE OF REPORT & PERIOD COVERED		
6 Electron Spectroscopic Studies of Surfaces and Interfaces for Adhesive Bonding	Final Report Jan. 77 - Aug. 79		
7. AUTHOR	8. CONTRACT OR GRANT NUMBER(s)		
10 Gerald E. Hammer and J.T./Grant	15 F33615-77-C-5040		
9. PERFORMING ORGANIZATION NAME AND ADDRESS	10. PROGRAM ELEMENT, PROJECT, TASK AREA & WORK UNIT NUMBERS		
Universal Energy Systems 3195 Plainfield Road Dayton, Ohio 45432	16 2303-Q1-02		
11. CONTROLLING OFFICE NAME AND ADDRESS	12. REPORT DATE		
Air Force Materials Laboratory (AFML/MBM) Air Force Wright Aeronautical Laboratories Wright Patterson AFB, Ohio 45433	17 January 1980		
14. MONITORING AGENCY NAME & ADDRESS (if different from Controlling Office)	13. NUMBER OF PAGES		
	76		
	15. SECURITY CLASS. (of this report)		
	Unclassified		
	15a. DECLASSIFICATION/DOWNGRADING SCHEDULE		
16. DISTRIBUTION STATEMENT (of this Report)			
Approved for public release; distribution unlimited			
17. DISTRIBUTION STATEMENT (of the abstract entered in Block 20, if different from Report)			
18. SUPPLEMENTARY NOTES			
19. KEY WORDS (Continue on reverse side if necessary and identify by block number)			
Auger Electron Spectroscopy Surface Analysis Adhesive Bonding X-ray photoelectron spectroscopy Electron Spectroscopy			
20. ABSTRACT (Continue on reverse side if necessary and identify by block number)			
This report summarizes the results from a thirty-one month research effort conducted to study the interaction of simple organic molecules on aluminum and titanium surfaces prepared for adhesive bonding using electron spectroscopic techniques. Other electron spectroscopic studies of specimens related to the surface phenomena program are also reported.			

DD FORM 1473

EDITION OF 1 NOV 65 IS OBSOLETE

SECURITY CLASSIFICATION OF THIS PAGE (When Data Entered)

JE 3

FOREWORD

This report describes the results of a research program undertaken to study surfaces and interfaces for adhesive bonding using electron spectroscopy. This report covers work performed during the period of January 1977 through June 1979 by Universal Energy Systems, Inc., 3195 Plainfield Road, Dayton, Ohio 45432 at the Air Force Materials Laboratory under contract F33615-77-C-5040, initiated under Task No. 2303Q1. The research was performed by G.E. Hammer, Dr. J.T. Grant and G.L. Jones with the technical assistance of R.G. Wolfe, J.R. Miller and L. Grazulis. The project engineer for the Air Force was Dr. T.W. Haas, Non metallic Materials Division (AFML/MBM). The authors submitted this report in September 1979.

Accession For	
NTIS GRA&I	<input checked="checked" type="checkbox"/>
DDC TAB	<input type="checkbox"/>
Unannounced	<input type="checkbox"/>
Justification	
By _____	
Distribution/	
Availability Codes	
Dist	Avail and/or special
A	

TABLE OF CONTENTS

SECTION	PAGE
I INTRODUCTION - - - - -	1
II ADSORPTION OF SIMPLE ORGANIC MOLECULES ON ANODIZED MATERIALS - - -	3
1. CHROMIC ACID ANODIZED AL - - - - -	5
2. PHOSPHORIC ACID ANODIZED AL - - - - -	13
3. CO-ADSORPTION WITH WATER ON PHOSPHIC ACID ANODIZED AL - - - -	16
III OTHER STUDIES RELATED TO ADHESIVE BONDING - - - - -	30
1. SMUT ON STAINLESS STEEL SURFACES - - - - -	-30
2. STRIPPABLE OXIDE FILMS - - - - -	30
3. AES/XPS COMPARISON OF ACID TREATED ALLOYS - - - - -	32
4. CORROSION STUDY OF PHOSPHONIC ANODIZED ALUMINUM - - - - -	32
5. XPS C 1s LINESHAPE STUDY ON AN ANODIZED ALUMINUM ADHESIVE SYSTEM - - - - -	32
IV DECONVOLUTION OF XPS SPECTRA - - - - -	38
V GRAPHITE FIBERS - - - - -	44
1. COMPARISON OF AS AND AU FIBERS USING Mg K _α RADIATION - - - -	44
2. COMPARISON OF HMS AND HMO FIBERS USING Mg K _α RADIATION - - - -	49
3. EFFECT OF VACUUM HEAT TREATMENT ON FIBERS - - - - -	51
4. FOREIGN MADE FIBERS - - - - -	62
VI SOLID LUBRICANT FILMS - - - - -	65
VII OTHER SURFACE STUDIES - - - - -	71
1. ELECTRON BOMBARDMENT OF BORON NITRIDE- - - - -	71
2. ANALYSIS OF ANGLE OF ATTACK TRANSMITTER - - - - -	71
3. ANALYSIS OF ANODIZED MERCURY CADMIUM TELLURIDE - - - - -	-72
APPENDIX A DECONVOLUTION PROGRAM FOR XPS DATA - - - - -	74
REFERENCES - - - - -	76

LIST OF ILLUSTRATIONS

FIGURE	PAGE
1 Carbon 1s XPS spectra of molecularly adsorbed (a) methanol and (b) acetone MoS ₂ . Spectrometer resolution was 1 eV.	4
2 XPS spectra of chromic acid anodized aluminum surface, (a) as prepared, and (b) after exposure to methanol at room temperature. Spectrometer resolution was 4 eV.	6
3 XPS spectra of chromic acid anodized aluminum surface, (a) after exposure to methanol at minus 100°C, and (b) after warming to room temperature. Spectrometer resolution was 4 eV.	7
4 Carbon 1s XPS spectra from chromic acid anodized aluminum (a) after cooling in vacuum, (b) following exposure to methanol at room temperature, (c) following exposure to minus 100°C, (d) after warming to room temperature and (e) methanol on MoS ₂ . Spectrometer resolution was 1 eV.	9
5 Oxygen 1s XPS spectra from chromic acid anodized aluminum (a) after cooling in vacuum, (b) following exposure to methanol at room temperature, (c) following exposure to methanol at minus 100°C, (d) after warming to room temperature and (e) methanol on MoS ₂ . Spectrometer resolution was 1 eV.	10
6 Carbon 1s XPS spectra from chromic acid anodized aluminum (a) after cooling in vacuum, (b) after exposure to methanol at 5×10^{-6} Pa for 2 min, (c) after further exposure to methanol at 1×10^{-5} Pa for 1 min, (d) after further exposure to methanol at 1×10^{-5} Pa for 5 min, and (e) after further exposure to methanol at 1×10^{-5} Pa for 5 min. Spectrometer resolution was 1 eV.	11
7 XPS spectra of phosphoric acid anodized aluminum, (a) as prepared, and (b) after exposure to methanol at 10^{-4} Pa for 300s at minus 100°C. Spectrometer resolution was 4 eV.	12
8 Carbon 1s XPS spectra from phosphoric acid anodized aluminum (a) after cooling in vacuum, (b) following exposure to methanol at room temperature, (c) following exposure to methanol at minus 100°C, (d) after warming to room temperature and (e) methanol on MoS ₂ . Spectrometer resolution was 1 eV.	14

LIST OF ILLUSTRATIONS (continued)

FIGURE		PAGE
9	Oxygen 1s XPS spectra from phosphoric acid anodized aluminum (a) after cooling in vacuum, (b) following exposure to methanol at room temperature, (c) following exposure to methanol at minus 100°C, (d) after warming to room temperature and (e) methanol on MoS ₂ . Spectrometer resolution was 1 eV.	15
10	XPS spectrum of phosphoric acid anodized aluminum, as prepared.	18
11	C 1s and O 1s spectra of phosphoric acid anodized aluminum, as prepared. Spectrometer pass energy was 65 eV.	19
12	C 1s and O 1s spectra of phosphoric acid anodized aluminum, after 16 hr exposure to water vapor in air. Spectrometer pass energy was 65 eV.	20
13	C 1s and O 1s spectra of phosphoric acid anodized aluminum after 16 hr exposure to formic acid and water vapors in air. Spectrometer pass energy was 65 eV.	21
14	C 1s and O 1s spectra of phosphoric acid anodized aluminum after 16 hr exposure to methanol and water vapors in air. Spectrometer pass energy was 65 eV.	23
15	C 1s and O 1s spectra of phosphoric acid anodized aluminum after 16 hr exposure to formaldehyde and water vapors in air. Spectrometer pass energy was 65 eV.	24
16	C 1s and O 1s spectra of phosphoric acid anodized aluminum after 16 hr exposure to formamide and water vapors in air. Spectrometer pass energy was 65 eV.	25
17	C 1s spectra of phosphoric acid anodized aluminum (a) as prepared and (b) after 10 min exposure to water vapor in air. Spectrometer pass energy was eV.	26
18	C 1s spectra of phosphoric acid anodized aluminum (a) as prepared and (b) after 10 min to formic acid and water vapors in air. Spectrometer pass energy was 65 eV.	27
19	C 1s spectra of phosphoric acid anodized aluminum (a) as prepared and (b) after 10 min exposure to methanol and water vapors in air. Spectrometer pass energy was 65 eV.	28
20	Analysis of Ta after stripping its oxide, (a) using Auger electron spectroscopy, and (b) using X-ray photoelectron spectroscopy.	31

LIST OF ILLUSTRATIONS (continued)

FIGURE	PAGE
21 AES spectra of anodized aluminum subjected to a corrosive atmosphere; (a) pitted area; (b) area near pit.	34
22 AES spectra of Al_2O_3 adhesive sample (a) sputtered into adhesive and (b) sputtered into anodized layer. Modulation was 5 eV peak-to-peak.	36
23 Carbon 1s XPS spectra of $Al-Al_2O_3$ - adhesive sample (a) sputtered into adhesive layer and (b) sputtered into anodized layer. Spectrometer resolution was 1 eV.	37
24 Calcium 2p XPS spectra, (a) raw data with a spectrometer resolution of 4 eV, (b) after 4 deconvolution approximations, (c) after 10 deconvolution approximations, and (d) raw data with a spectrometer resolution of 1 eV.	41
25 Chlorine 2p XPS spectra, (a) raw data with a spectrometer resolution of 1 eV, and (b) after 5 deconvolution approximations.	42
26 XPS spectra of graphite fibers, (a) AU type fibers, and (b) AS type fibers. Spectrometer resolution was 4 eV.	45
27 XPS spectra of graphite fibers, (a) HMU type fibers, and (b) HMS type fibers. Spectrometer resolution was 4 eV.	50
28 Carbon 1s XPS spectra from, (a) AS type fibers, and (b) from HMU type fibers. Spectrometer resolution was 1 eV.	52
29 XPS spectra of AU type graphite fibers (a) after 300°C vacuum heat treatment and (b) as received. Spectrometer resolution was 4 eV.	53
30 XPS spectra of AS type graphite fibers (a) after 300°C vacuum heat treatment and (b) as received. Spectrometer resolution was 4 eV.	54
31 XPS spectra of HMU type graphite fibers (a) after 300° vacuum heat treatment and (b) as received. Spectrometer resolution was 4 eV.	55
32 XPS spectra of HMS type graphite fibers (a) after 300°C vacuum heat treatment and (b) as received. Spectrometer resolution was 4 eV.	56
33 Carbon 1s XPS spectra of AS fiber (a) after 300°C vacuum heat treatment and (b) as received. Spectrometer resolution was 2 eV.	59

LIST OF ILLUSTRATIONS (continued)

FIGURE		PAGE
34	Oxygen 1s spectra of AS fiber (a) after 300°C vacuum heat treatment and (b) a received. Spectrometer resolution was 2 eV.	60
35	Carbon 1s XPS spectra from (a) AS7H, (b) ASV6, and (c) AS graphite fibers. Spectrometer resolution was 2 eV.	63
36	Auger electron spectrum from foreign made fibers. Electron beam energy was 3 keV, time constant 0.3s and modulation (sinusoidal) 6 eV peak-to-peak.	64
37	Analysis of co-sputtered MoS ₂ and Sb ₂ O ₃ using (a) Auger electron spectroscopy, and (b) x-ray photoelectron spectroscopy.	66
38	XPS spectra from, (a) MoS ₂ + Sb ₂ O ₃ burnished film, and (b) partly oxidized InSb. Spectrometer resolution was 1 eV.	67
39	Molybdenum 3d XPS spectra from two partly worn gas bearings, (a) and (b). Spectrometer resolution was 1 eV.	68
40	Molybdenum 3d XPS spectra from, (a) air oxidized molybdenum, (b) burnished MoS ₂ film, and (c) clean molybdenum. Spectrometer resolutions was 1 eV.	70
41	AES depth profile of anodized Hg Cd Te. Modulation was 6 eV peak-to-peak.	73

LIST OF TABLES

TABLE	PAGE
1 Relative surface concentrations of elements from a 7075 Aluminum alloy obtained from AES and XPS. _ _ _ _ _	33
2 Measured full widths at half maximum (FWHM for C, O, Na, and N 1s Photoelectron Peaks from As and AU fibers. _ _ _ _ _	47
3 Concentration in Atomic per cent in Graphite Fibers: Calculated from 1s Peak Heights Under 4eV Resolution. _ _ _ _ _	48
4 Concentration in Atomic per cent in Graphite Fibers: Calculated from 1s Peak Areas under 1eV Resolution. _ _ _ _ _	48
5 Concentration in Atomic per cent in Graphite Fibers: Calculated from 1s Peak Areas under 2eV Resolution. _ _ _ _ _	57
6 Concentrations in Atomic per cent in Graphite Fibers: Calculated from 1s Peak Areas under 2eV Resolution. _ _ _ _ _	61

SECTION I

INTRODUCTION

The use of adhesive bonding in joining both primary and secondary structural components of aircraft and spacecraft has many potential advantages such as reduced weight, reduced machining, material and assembly cost, efficient transfer of loads between components, a reduction in problems associated with stress corrosion in and around rivets that lead to fatigue cracking, etc. Further, missiles and spacecraft could hardly exist without the use of adhesives as, for example, the attachment of ablative heat shields to metallic substructures can be made only with adhesives. Because of many significant advantages of adhesive bonding as a joining technique there is a definite need to conduct research in this area, particularly with a view to improved durability, reliability, reproducibility, and predictability of failure. One extremely important area for research is the study of the strength of bonding between the adhesive and the adherend, including long term effects such as moisture degradation, phase changes in the anodized layer, and polymer decomposition. The control and predicatability of such effects require an understanding of how organic molecular functional groups interact with surfaces prepared for adhesive bonding.

This report describes the work carried out during a 31 month contract to study the interaction of simple organic molecules such as methanol, acetone, formic acid, and methylamine on aluminum and titanium surfaces prepared for adhesive bonding using electron spectroscopic techniques. The effect of the coadsorption of water with these organics has also been studied. The results obtained using Auger Electron Spectroscopy (AES and X-ray Photo-electron Spectroscopy (XPS are reported in Section II.

Related Studies of other adhesive bonding samples are included in Section III. A deconvolution program to eliminate the effects of spectrometer broadening and X-ray line shape in XPS data has been developed and is described in Section IV.

A study of the effects of surface preparation and treatment on graphite fibers used in composite materials is reported in Section V.

Other electron spectroscopic studies of specimens related to the surface phenomena program are reported in Sections VI and VII.

SECTION II

ADSORPTION OF SIMPLE ORGANIC MOLECULES ON ANODIZED MATERIALS

In order to study the adsorption and interaction of simple organic molecules on anodized materials, reference XPS spectra of adsorbed, non-decomposed organic molecules are required. A suitable substrate for obtaining such reference spectra is molybdenum disulfide which has no unsatisfied bonds on a perfect cleavage surface and is very inert. Therefore, molecular adsorption can occur on MoS_2 at low temperatures. To carry out this phase of the work a cold stage for cooling specimens was designed and constructed. By cooling with liquid nitrogen, specimen temperatures down to minus 100°C were obtained.

One problem was noted in cleaning the cleaved MoS_2 surfaces. Inert gas sputtering removed surface contaminants (carbon and oxygen), but also selectively sputtered sulfur, resulting in a sulfur deficient molybdenum disulfide. When acetone was adsorbed on this surface only one carbon XPS peak was found indicating that the acetone had decomposed. This problem was resolved by cleaning the cleaved MoS_2 by heating in the ultra high vacuum system. A surface having the calculated composition of MoS_2 was then obtained and molecular adsorption of acetone was achieved. Reference carbon 1s XPS spectra of molecularly adsorbed methanol and acetone are shown in Figure 1 (a) and (b) respectively. Note that the two carbon 1s lines from the acetone have an intensity ratio of 1:2 corresponding to the two valence states of carbon in acetone. A dummy run was carried out to see if any carbon containing background gases in the vacuum system adsorbed on the cooled MoS_2 during analysis - none were observed to

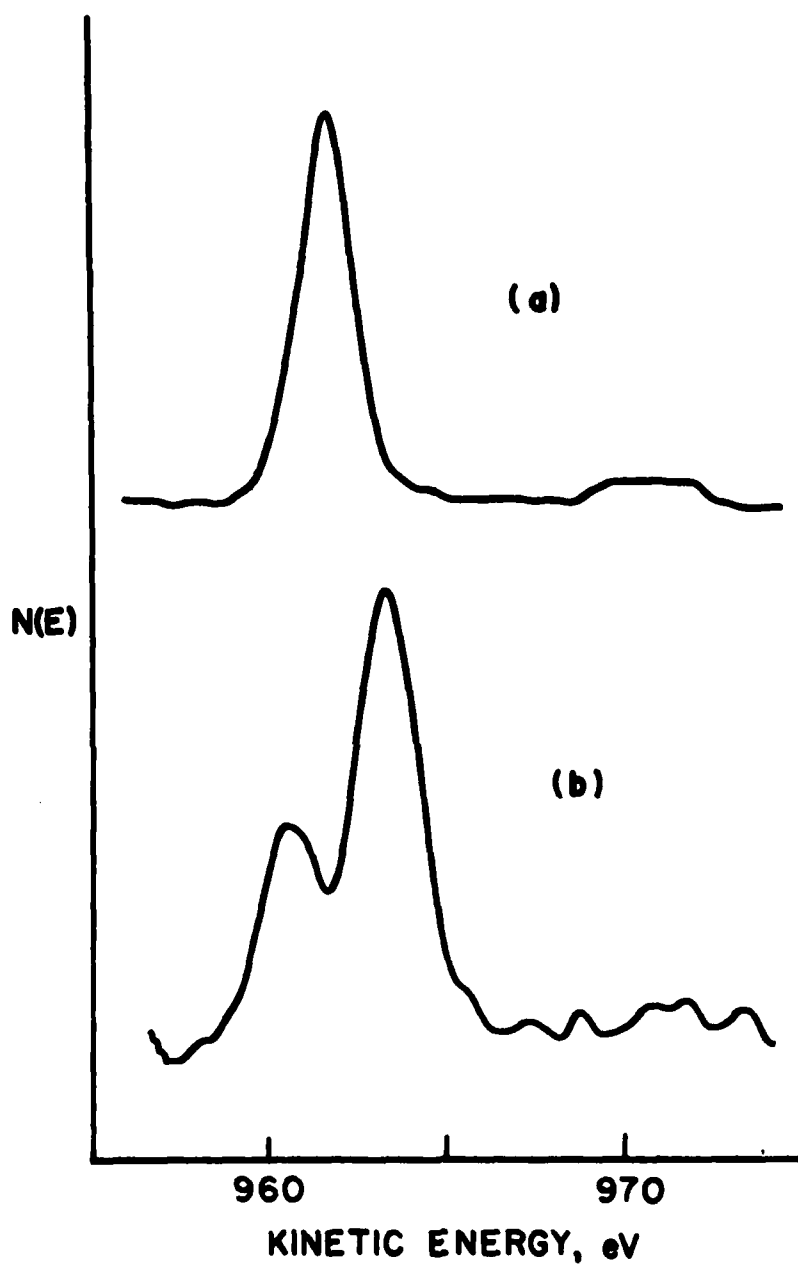


FIGURE 1 - Carbon 1s XPS spectra of molecularly adsorbed (a) methanol and (b) acetone on MoS_2 . Spectrometer resolution was 1 eV.

adsorb. Cooling MoS_2 to minus 100°C in 5×10^{-3} Pa of CO and CO_2 also produced no adsorption (limit of detectability being 2% of a monolayer).

The first adsorption studies carried out were the adsorption of methanol on phosphoric acid and chromic acid anodized aluminum. These two anodization methods were chosen because of the different corrosion resistances (to water) and different porosities of the anodized layers - the phosphoric acid anodized specimens have the better corrosion resistance and larger pores.

1. CHROMIC ACID ANODIZED AL

An XPS spectrum from a chromic acid anodized Al surface is shown in Figure 2 (a). Note that besides Al and O, C, N, F, and Cr are detected. The chromium comes from the anodization bath, whereas the N and F remain from the pickling procedure (a mixture of HF and HNO_3) before anodization. Exposure of this specimen to methanol at 10^{-4} Pa for 300s (the pressures reported being uncorrected nude ionization gauge readings) did not show any significant adsorption, Figure 2 (b). However, after cooling the specimen to minus 100°C in 10^{-4} Pa of methanol (it takes about 15 min to cool the specimen) and further exposing it for another 15 min at this temperature, adsorption did occur as can be seen in the XPS spectrum shown in Figure 3 (a). Note that the substrate features (e.g., Al) are no longer detected due to adsorption. The nitrogen peak may arise due to a small air leak in the cold stage. This spectrum was taken with the specimen held at minus 100°C after evacuating the methanol from the UHV chamber. After the specimen was allowed to warm to room temperature the XPS spectrum shown in Figure 3 (b) was obtained indicating that the methanol adsorption was reversible. The oxygen to carbon concentrations were calculated using the carbon and oxygen 1s peak heights in these 4eV

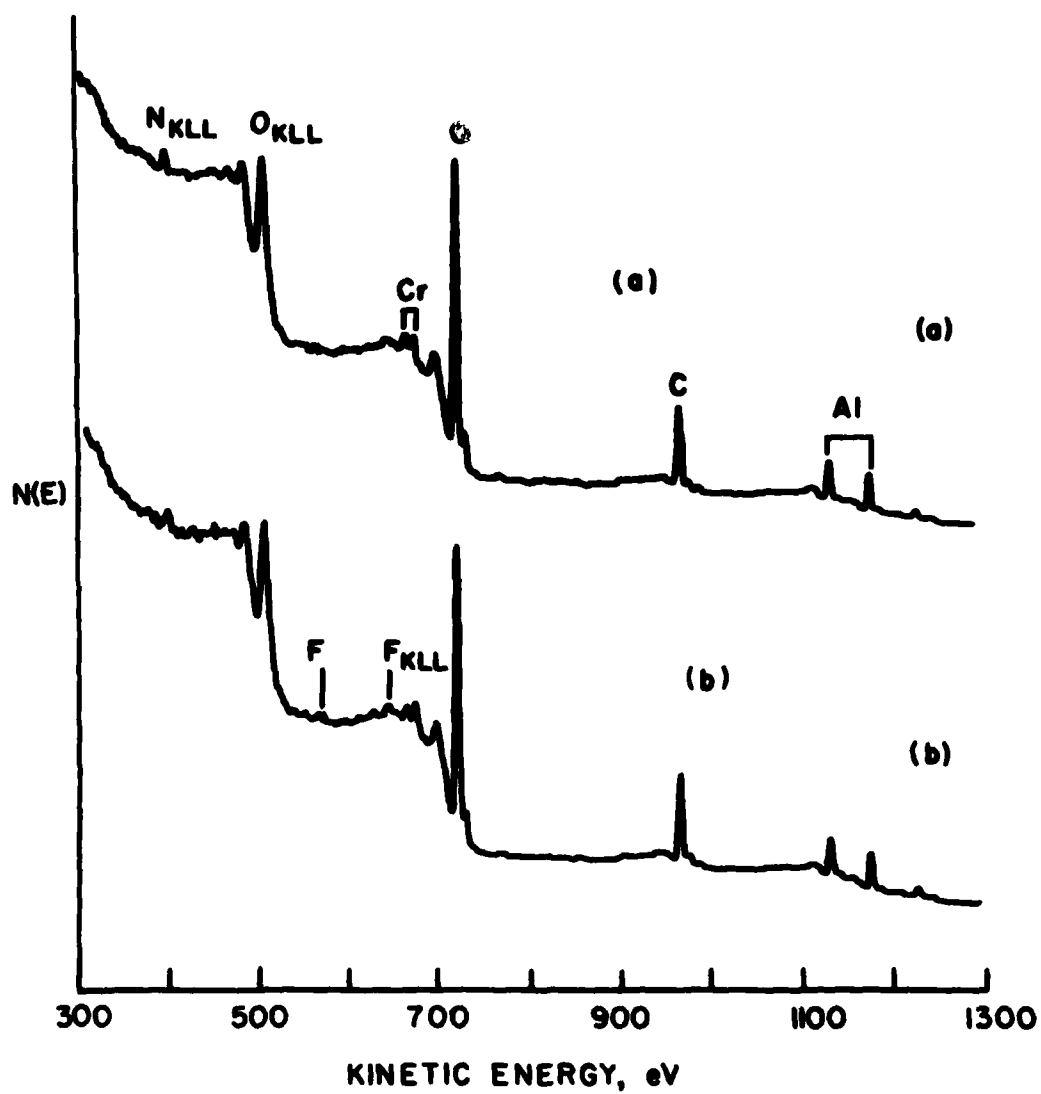


FIGURE 2 - XPS spectra of chromic acid anodized aluminum surface, (a) as prepared, and (b) after exposure to methanol at room temperature. Spectrometer resolution was 4 eV.

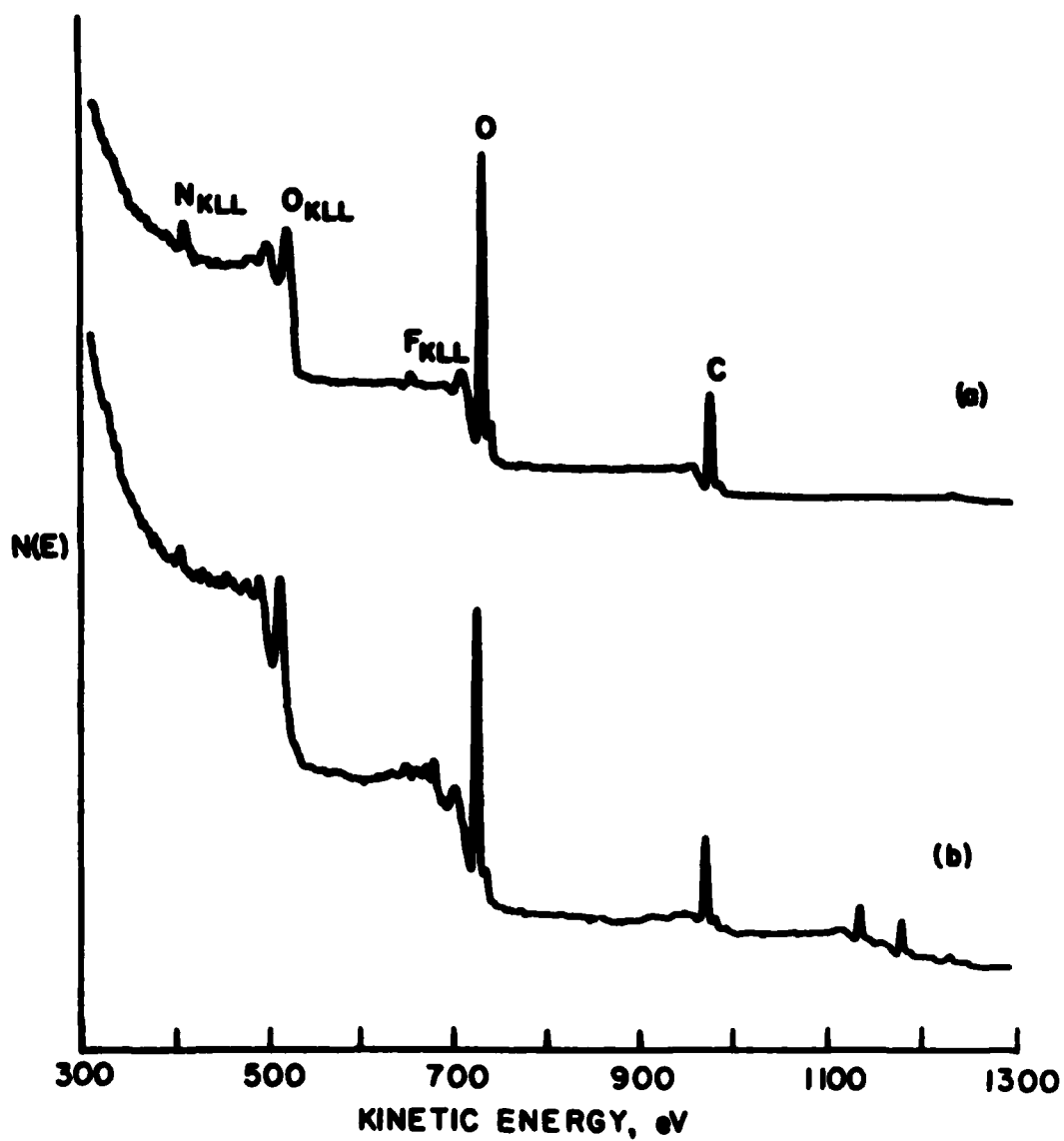


FIGURE 3 - XPS spectra of chromic acid anodized aluminum surface, (a) after exposure to methanol at minus 100°C, and (b) after warming to room temperature. Spectrometer resolution was 4 eV.

resolution spectra, Figures 2 and 3, and using Scofield¹ cross sections for the 1s levels. Before adsorption, the carbon to oxygen ratio was 1.3, on exposure to methanol at room temperature 1.1, on exposure at minus 100°C 1.1, and after warming to room temperature 1.1. The changes in these ratios are rather small and probably not significant. The ratio obtained for methanol on MoS₂ was 1.0 so it is not possible to detect the adsorption of methanol from such data as the oxygen to carbon concentration was so close to 1.0 before adsorption.

High resolution carbon 1s, oxygen 1s and aluminium 2p XPS spectra were also taken during the different stages of adsorption (1 eV spectrometer resolution). The aluminum 2p peak had a FWHM of about 2.2 eV before and after exposure. The carbon and oxygen 1s spectra are shown in Figures 4 and 5 respectively, together with the spectra for methanol on MoS₂. The C and O peak energies and widths before and after adsorption are quite similar whereas an adsorption at minus 100°C the peaks are shifted to higher kinetic energies and the O width was slightly reduced, from 2.8 eV to 2.2 eV. The difference in kinetic energies between C and O peaks was constant at 245.5 ± 0.3 eV for all the spectra and as the C and O widths on methanol adsorption were larger than the reference spectra it was felt that the specimen was charging electrically for the data shown in Figure 4 (c) and 5 (c). To check for charging, another adsorption run was made with the specimen held at minus 100°C and exposed to lower concentrations of methanol. The carbon 1s spectra obtained from the experiment are shown in Figure 6. Here the growth of a new C peak, on the low kinetic energy side of the C peak obtained from the anodized substrate, is quite apparent with increasing methanol exposure. This

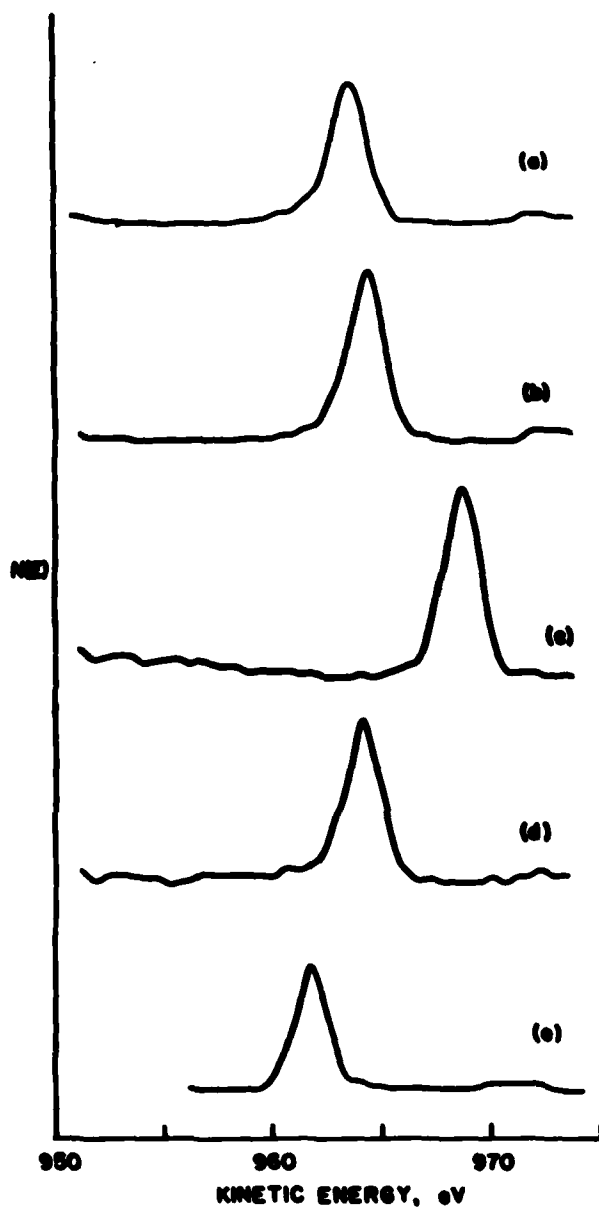


FIGURE 4 - Carbon 1s XPS spectra from chromic acid anodized aluminum (a) after cooling in vacuum, (b) following exposure to methanol at room temperature, (c) following exposure to methanol at minus 100°C, (d) after warming to room temperature and (e) methanol on MoS₂. Spectrometer resolution was 1 eV.

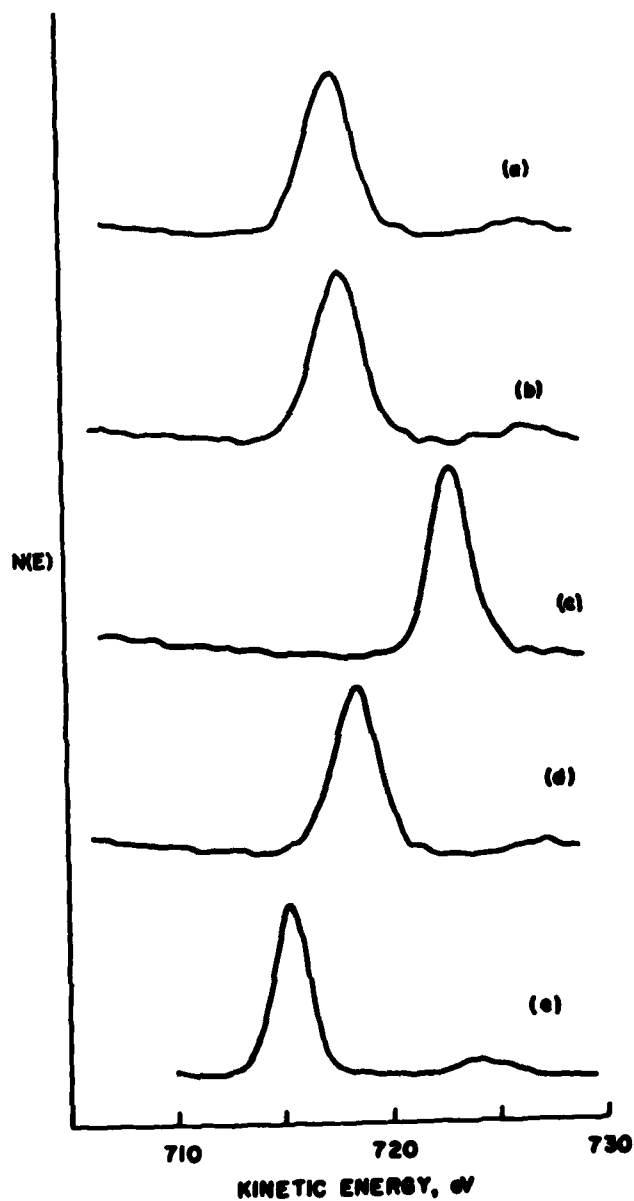


FIGURE 5 - Oxygen 1s XPS spectra from chromic acid anodized aluminum (a) after cooling in vacuum, (b) following exposure to methanol at room temperature, (c) following exposure to methanol at minus 100°C, (d) after warming to room temperature and (e) methanol on MoS₂. Spectrometer resolution was 1 eV.

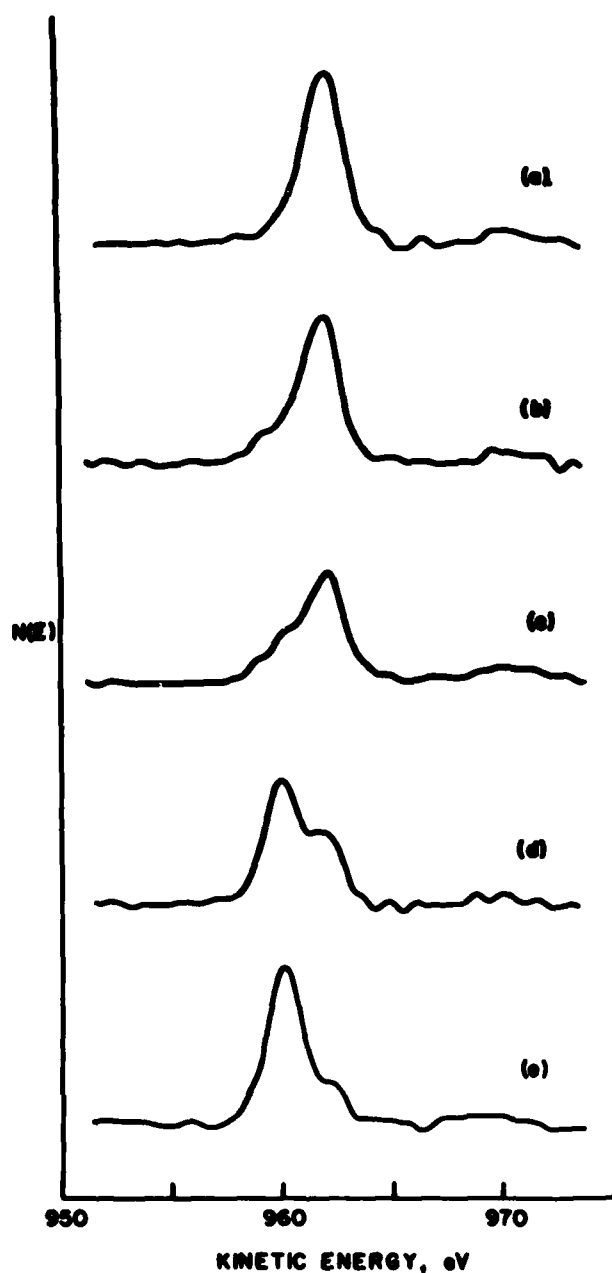


FIGURE 6 - Carbon 1s XPS spectra from chromic acid anodized aluminum (a) after cooling in vacuum, (b) after exposure to methanol at 5×10^{-6} Pa for 2 min, (c) after further exposure to methanol at 1×10^{-5} Pa for 1 min, (d) after further exposure to methanol at 1×10^{-5} Pa for 5 min, and (e) after further exposure to methanol at 1×10^{-5} Pa for 5 min. Spectrometer resolution was 1 eV.

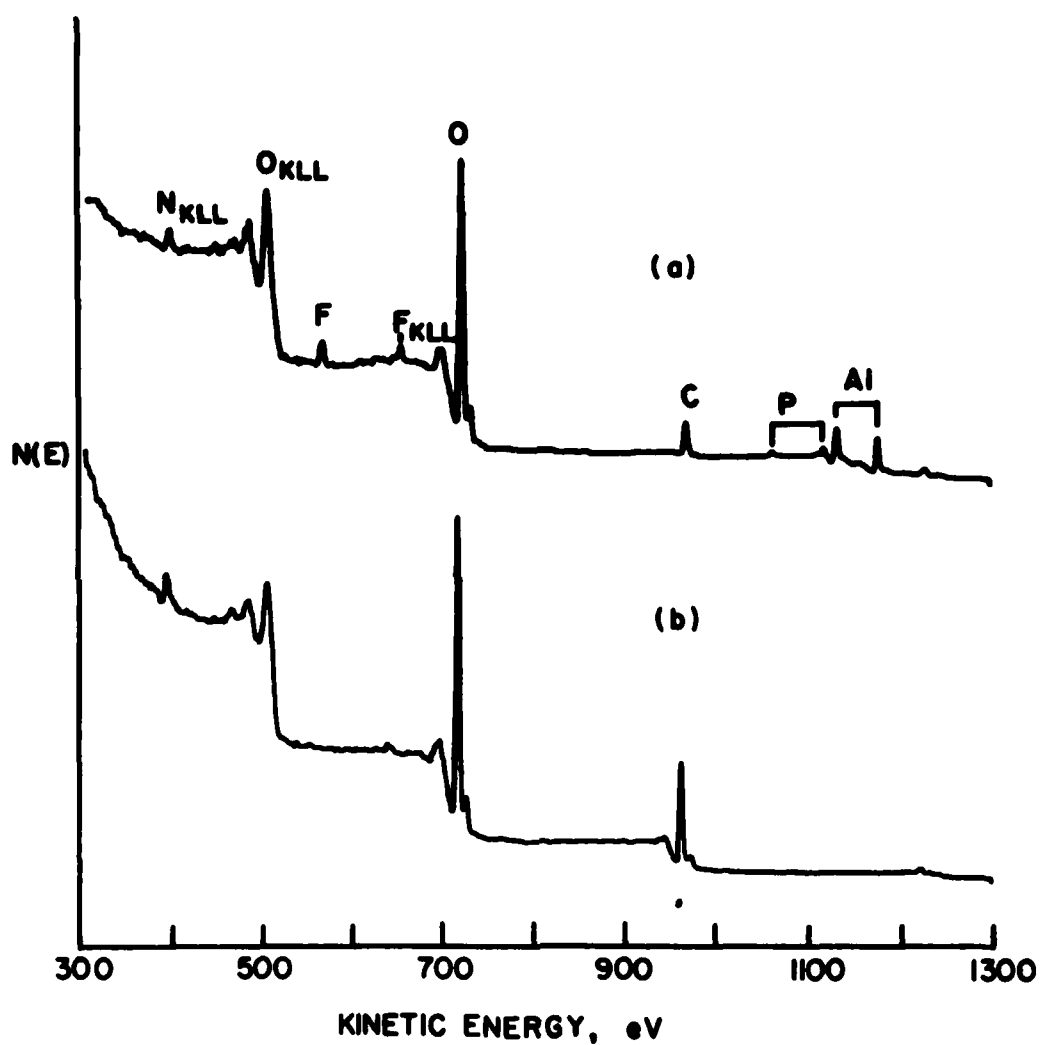


FIGURE 7 - XPS spectra of phosphoric acid anodized aluminum, (a) as prepared, and (b) after exposure to methanol at 10^{-4} Pa for 300s at minus 100°C . Spectrometer resolution was 4 eV.

C peak is shifted 2.0 eV from the substrate peak and appears at an energy close to that for methanol on MoS_2 . This C peak also has a FWHM of about 2.0 eV, close to that for methanol MoS_2 , 1.8 eV. Such problems due to specimen charging often occur in electron spectroscopy and can result in erroneous interpretations if care is not exercised in interpreting data.

2. PHOSPHORIC ACID ANODIZED AL

An XPS spectrum from phosphoric acid anodized Al is shown in Figure 7 (a). Note the presence of phosphorus, due to the anodization bath. Exposure of this specimen to 10^{-4} Pa of methanol for 300s also did not result in any significant adsorption. However, on cooling the specimen to minus 100°C, adsorption did occur and the corresponding XPS spectrum is shown in Figure 7 (b). Again, note the disappearance of the substrate peaks. On allowing the specimen to warm to room temperature the methanol desorbed.

Oxygen to carbon concentrations were also calculated from these spectra. Before adsorption the carbon to oxygen was 2.7, on exposure to methanol at room temperature 3.4, on exposure at minus 100°C 1.1, and after warming to room temperature 2.9. Unlike the corresponding data for the chromic acid anodized specimen where all ratios were close to unity, the adsorption of methanol on this specimen can clearly be identified from the calculated oxygen to carbon concentration.

High resolution carbon 1s, oxygen 1s and aluminum 2p XPS spectra were also taken during the different stages of adsorption. Again, the aluminum 2p peak had a FWHM of about 2.2 eV before and after exposure. The carbon and oxygen 1s spectra are shown in Figures 8 and 9 respectively, together with the spectra for methanol on MoS_2 . Both the carbon and

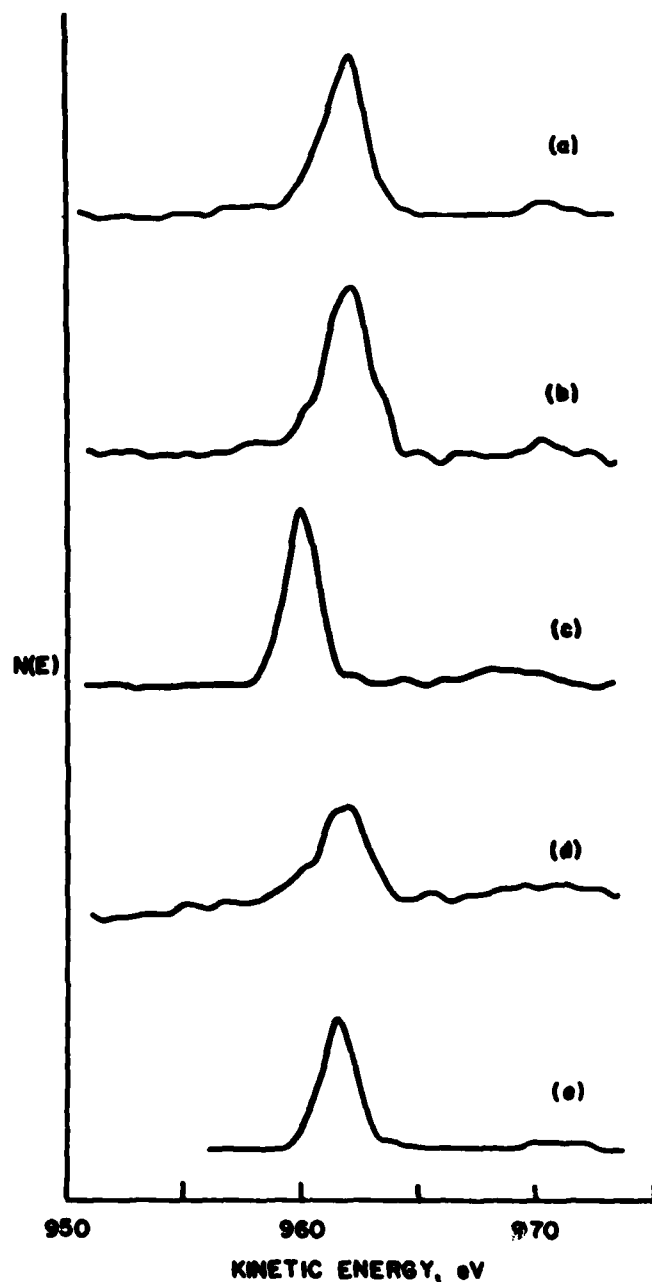


FIGURE 8 - Carbon 1s XPS spectra from phosphoric acid anodized aluminum (a) after cooling in vacuum, (b) following exposure to methanol at room temperature, (c) following exposure to methanol at minus 100°C, (d) after warming to room temperature and (e) methanol on MoS₂. Spectrometer resolution was 1 eV.

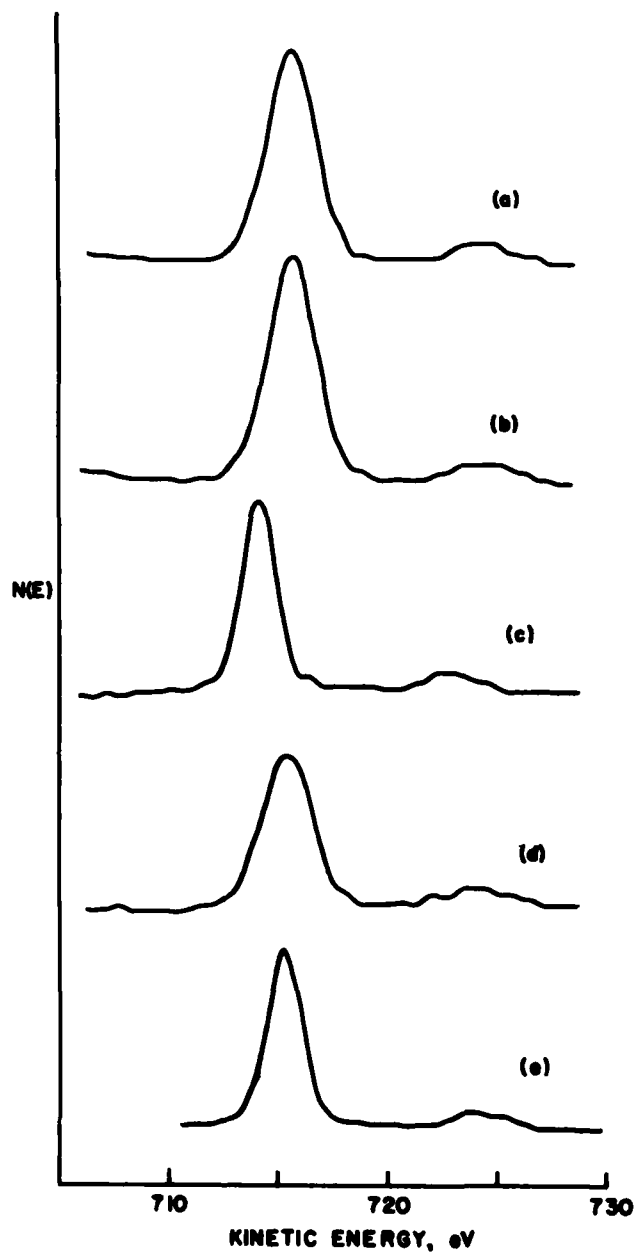


FIGURE 9 - Oxygen 1s XPS spectra from phosphoric acid anodized aluminum, (a) after cooling in vacuum, (b) following exposure to methanol at room temperature, (c) following exposure to methanol at minus 100°C, (d) after warming to room temperature and (e) methanol on MoS₂. Spectrometer resolution was 1 eV.

oxygen XPS lines are narrower following methanol adsorption and have the same widths as methanol on MoS_2 . The kinetic energies of the peaks are slightly lower than for methanol on MoS_2 and this difference (1 eV) may be due to a small amount for electrical charging. After desorption the wider carbon and oxygen lines from the anodized specimen reappear.

Similar studies were performed exposing anodized aluminum surfaces to acetone and again only molecular adsorption on cooled substrates was observed. A turbomolecularly pumped sample preparation chamber (base pressure 1×10^{-5} Pa) was added to the system and in it phosphoric acid anodized aluminum samples were exposed to ethylene oxide and monomethylamine at pressures of 5×10^{-3} Pa, and 1.33 Pa and 13.3 Pa. No evidence of adsorption at room temperature of these organics was observed.

In conclusion, it appears that the interaction of the organics studied with chromic and phosphoric acid anodized Al is very weak, as all that has been observed is molecular adsorption at low temperatures.

3. CO-ADSORPTION WITH WATER ON PHOSPHORIC ACID ANODIZED AL

These studies were all performed on samples which were etched for 10 minutes in a solution of 25g HF and 125g HNO_3 in 1l water, rinsed in distilled water, anodized in 1M phosphoric acid at 20v for 5 minutes, again rinsed in distilled water, then allowed to dry in air. The starting material was 99.99% pure Al.

A new XPS system was used and it produced higher sensitivity and resolution than the system used in the early work. The base pressure of the new system was 2×10^{-7} Pa, and a differentially pumped sample insertion lock allowed a sample to be introduced into the chamber for analysis with the system pressure returning to $< 5 \times 10^{-7}$ Pa (where the

analysis was performed) in less than 1 hour.

After a sample was prepared and inserted into the vacuum chamber and working pressure obtained, a broad (0 to 1250 eV) scan was recorded. A typical spectrum is shown in Figure 10. As adsorption of the organic material being studied would be indicated by changes in the carbon or oxygen 1s lines, high resolution spectra of these lines were also recorded; typical spectra are shown in Figure 11. High resolution spectra of the other major peaks were also recorded to insure uniformity among the samples as prepared. Corrected peak area measurements indicated a carbon atomic concentration of about 5%.

The sample was then withdrawn from the vacuum system and placed in a clear glass beaker which also held smaller beakers, one containing about 5 ml of distilled water and the other 5 ml of the organic being studied. The beaker was then sealed, and the sample was therefore exposed to the vapor of the organic along with water vapor in air at room temperature.

For the initial, the samples were exposed overnight (16 hrs). The first exposure was performed with water only in the beaker to determine the effects of the adsorption of carbon and oxygen containing contaminants from the water and in the air. High resolution XPS spectra taken after a 16 hr exposure to water vapor in air are shown in Figure 12. The only obvious changes are an increase in the total carbon signal and the appearance of a weak higher binding energy peak around 292 eV.

The second study was performed with formic acid as well as water vapor in the beaker. Spectra taken after a 16 hr exposure are shown in Figure 13. The increase in the total carbon signal was much greater in

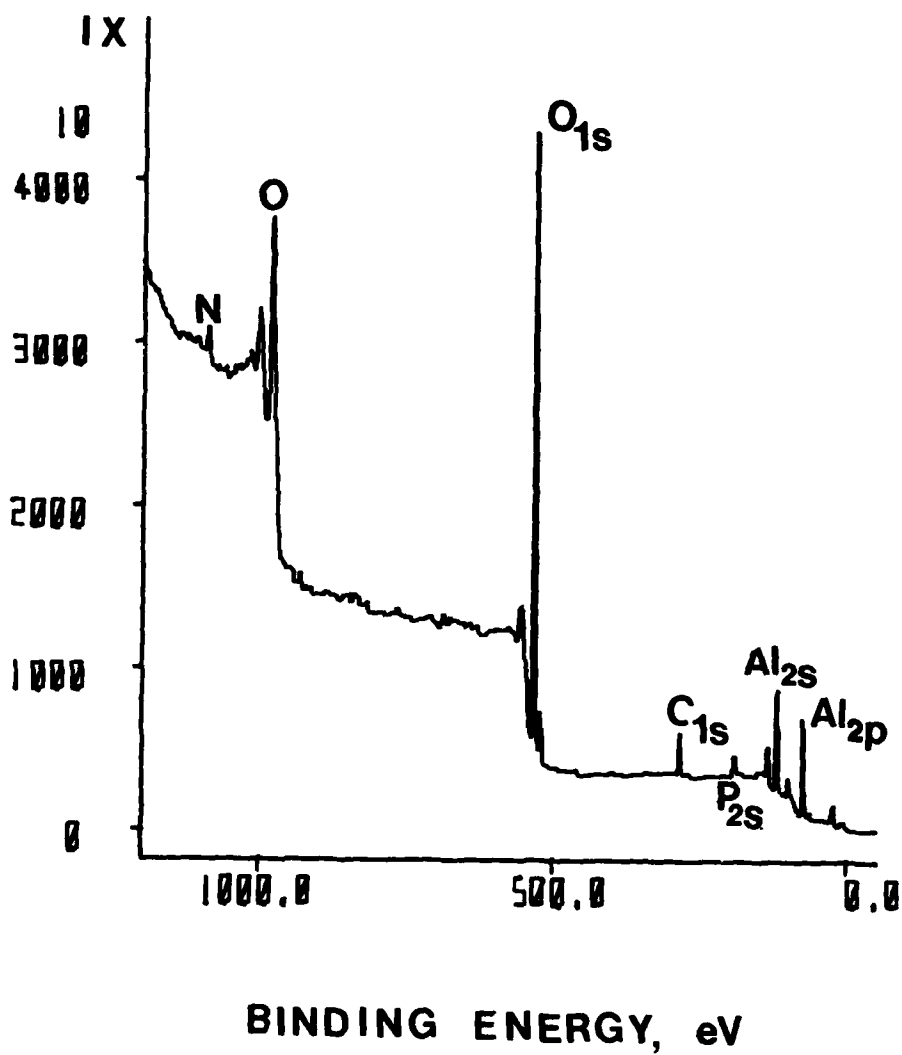


FIGURE 10 - XPS spectrum of phosphoric acid anodized aluminum, as prepared.

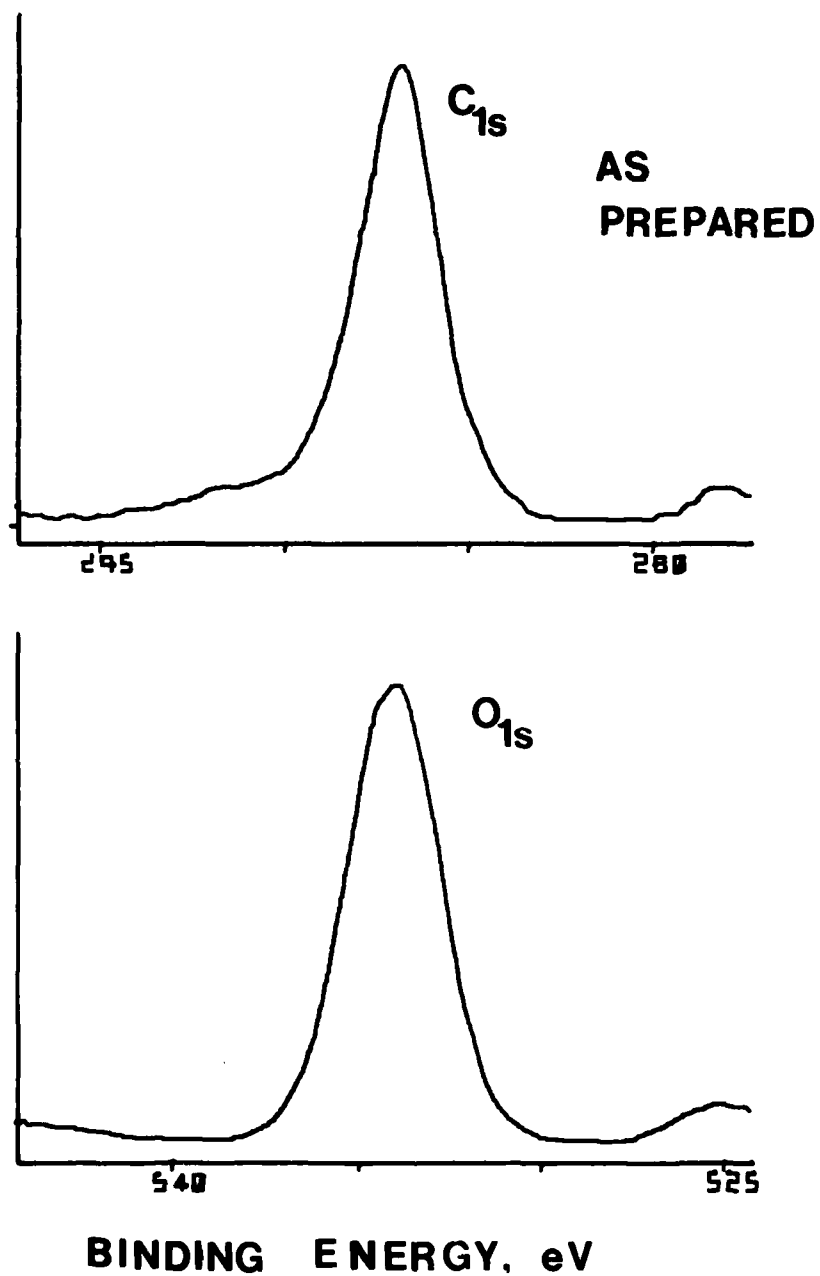


FIGURE 11 - C_{1s} and O_{1s} spectra of phosphoric acid anodized aluminum, as prepared. Spectrometer pass energy was 65 eV.

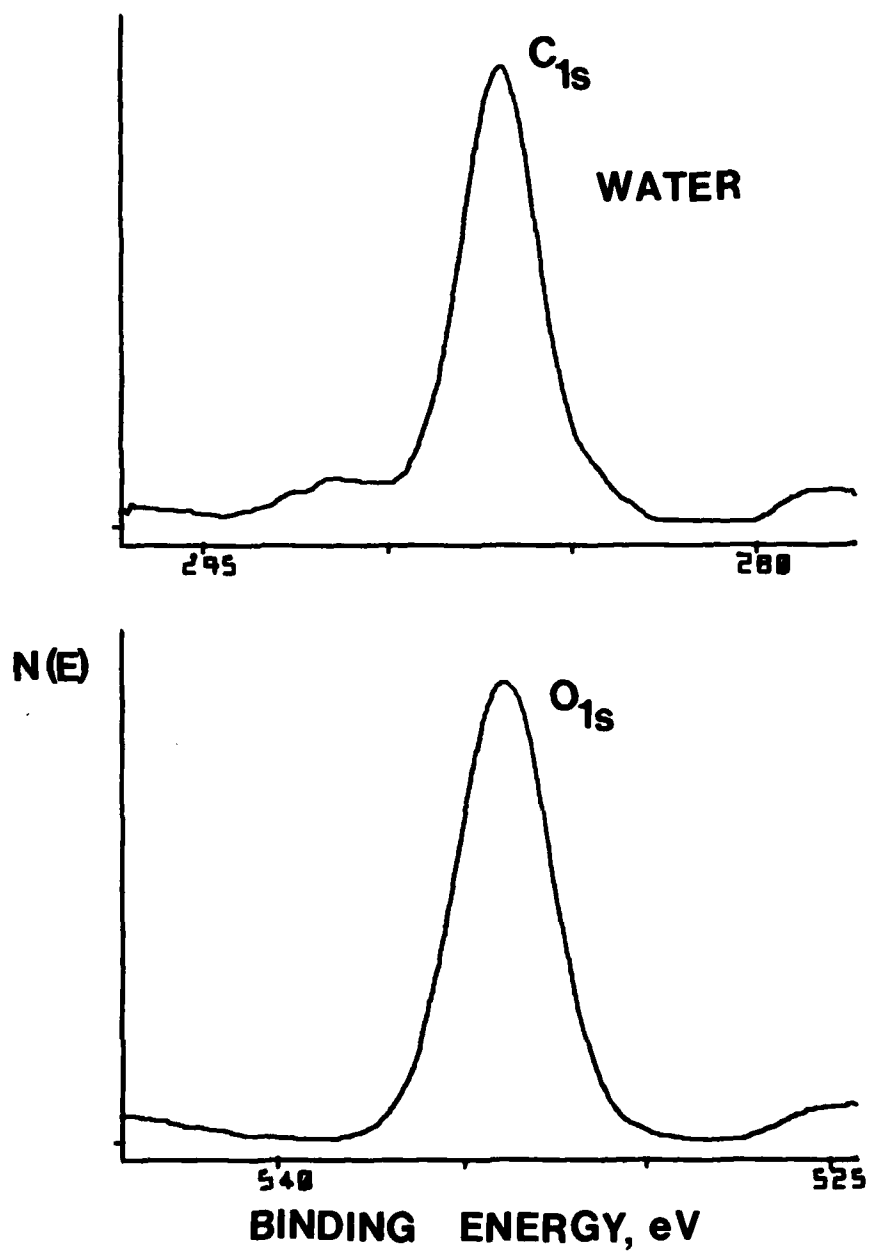


FIGURE 12 - C 1s and O 1s spectra of phosphoric acid anodized aluminum, after 16 hr exposure to water vapor in air. Spectrometer pass energy was 65 eV.

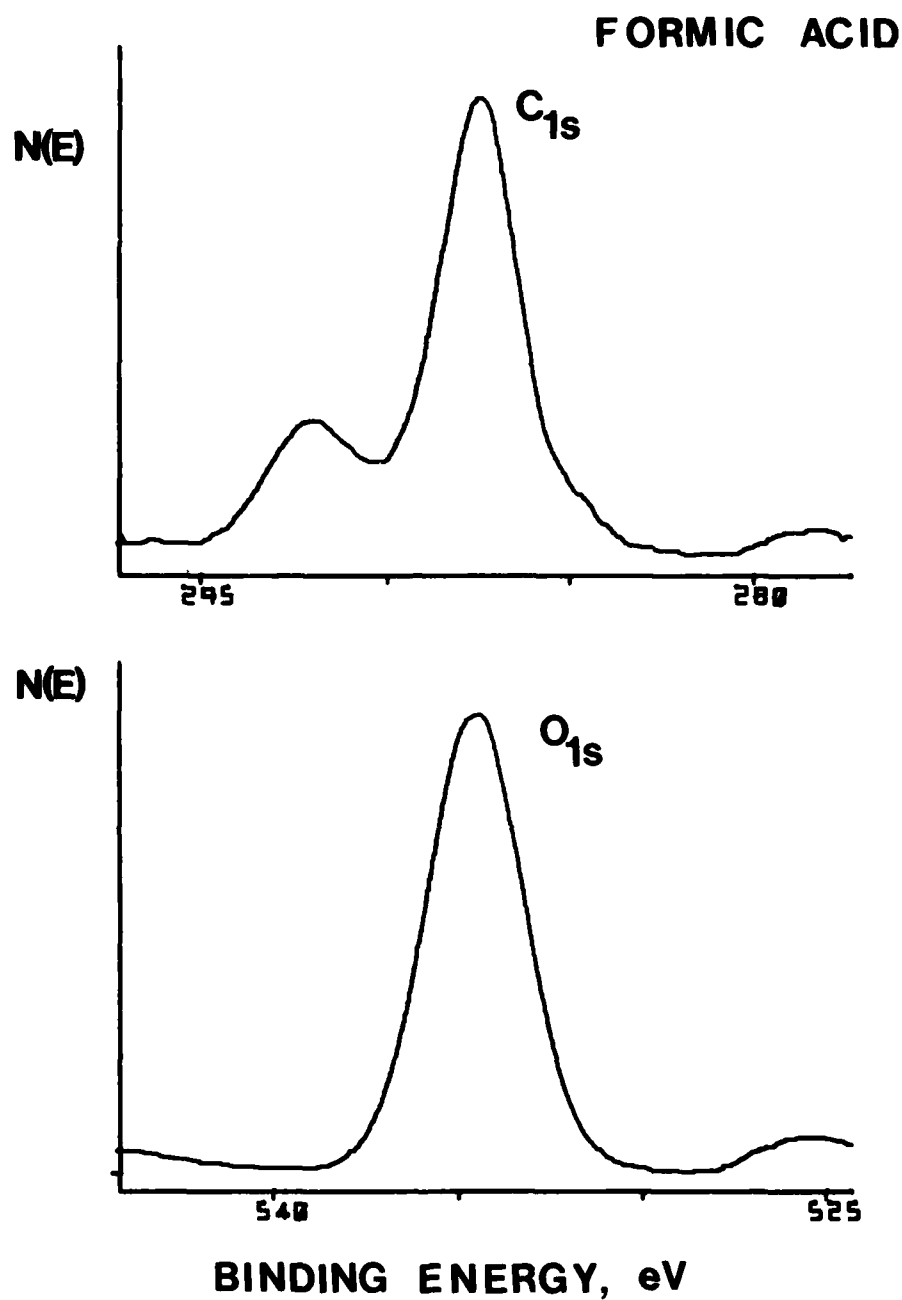


FIGURE 13 - C 1s and O 1s spectra of phosphoric acid anodized aluminum after 16 hr exposure to formic acid and water vapors in air. Spectrometer pass energy was 65 eV.

this case and the high binding energy peak (around 292 eV) is much stronger. These two observations, the second one in particular appear to indicate that the formic acid has adsorbed onto the aluminum oxide surface.

The experiment was then repeated using methanol, formaldehyde, and formamide. The results are shown in Figures 14, 15, and 16. All show, to a greater or lesser extent, a proportionately large increase in the resulting signal strength from a high binding energy carbon peak, indicating for each some degree of adsorption onto the aluminum oxide.

To get some indication of the rate at which the adsorption was taking place and possibly reduce the effects of contaminants, a series of exposures of 10 minutes was performed. At the end of the exposure period the samples were (as before) immediately mounted on the sample holder and inserted into the vacuum system. High resolution C_{1s} spectra of the as prepared sample and after 10 minutes exposure to water vapor are shown in Figure 17 (a) and (b), respectively. Only a slight increase in the peaks is observed.

Corresponding spectra for a sample exposed to water and formic acid vapor are shown in Figures 18 (a) and (b). Significant increases in both the main carbon peak and the high binding energy peak are observed. Similar, but not quite as large changes appear for a sample exposed to methanol and water vapor for 10 minutes, Figures 19 (a) and (b).

In conclusion we can say that although the phosphoric anodized aluminum surface appears to be inert to these organic molecules by themselves, adsorption does take place in the presence of water.

This is most clearly illustrated by the results with methanol,

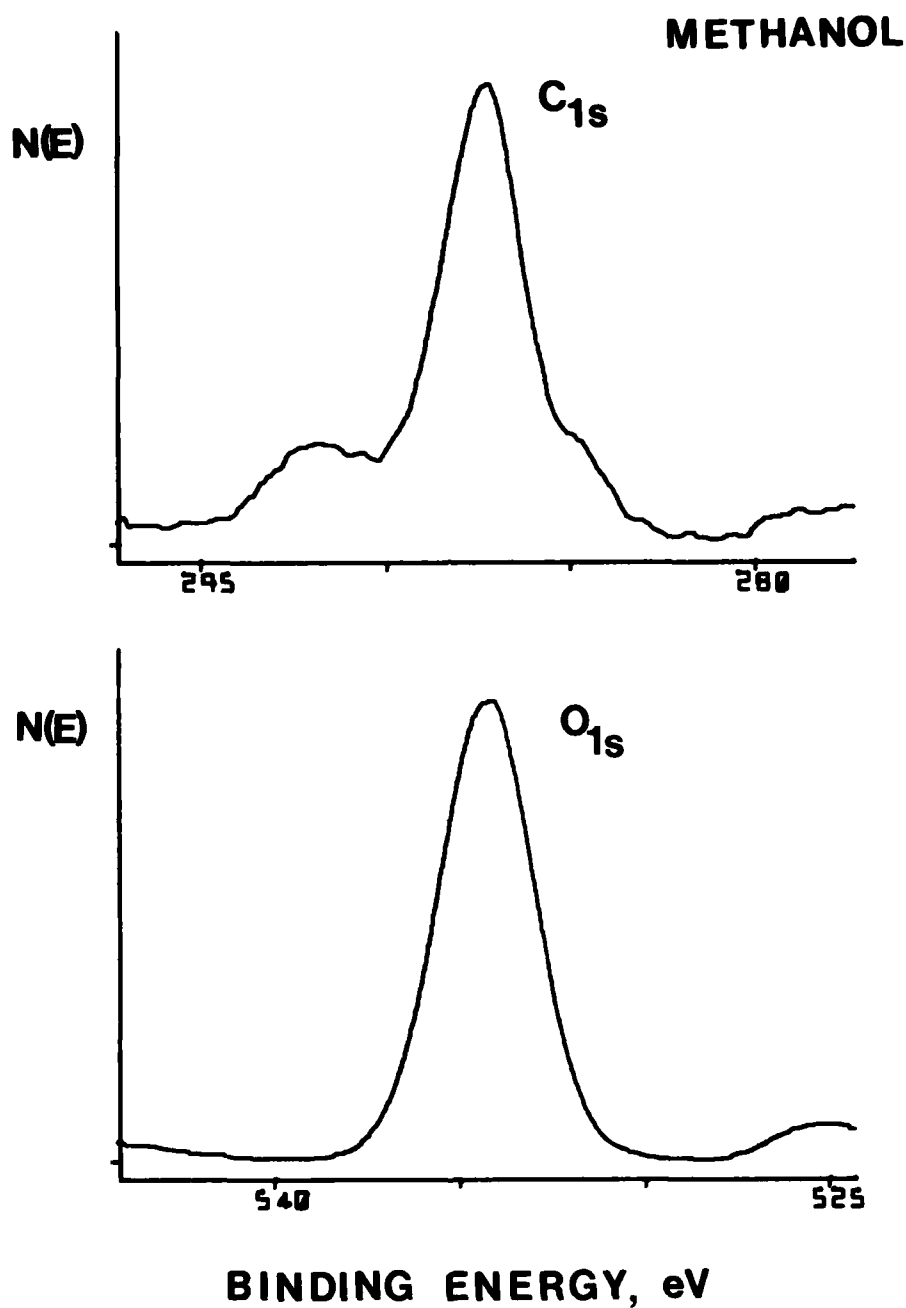


FIGURE 14 - C_{1s} and O_{1s} spectra of phosphoric acid anodized aluminum after 16 hr exposure to methanol and water vapors in air. Spectrometer pass energy was 65 eV.

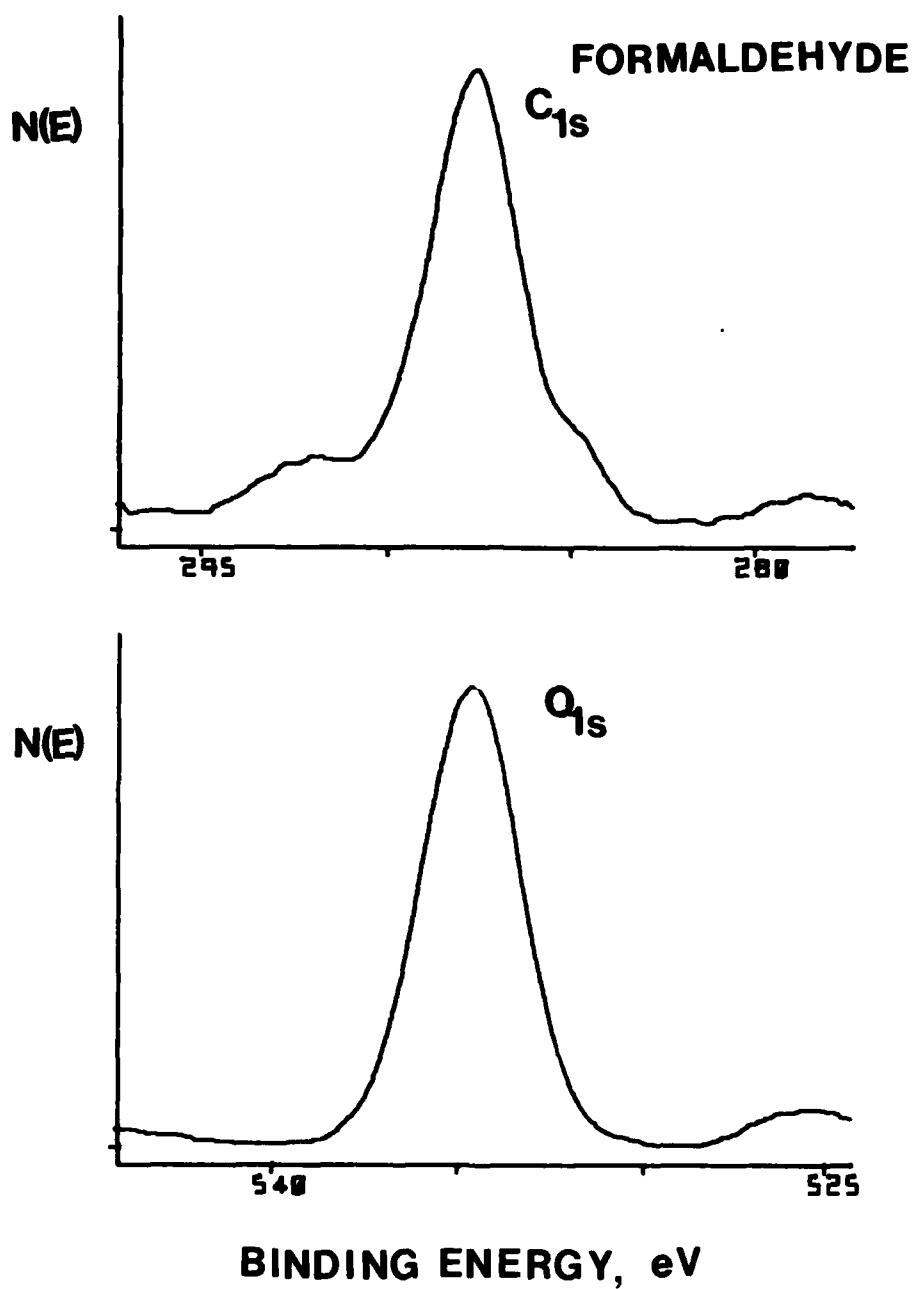


FIGURE 15 - C 1s and O 1s spectra of phosphoric acid anodized aluminum after 16 hr exposure to formaldehyde and water vapors in air. Spectrometer pass energy was 65 eV.

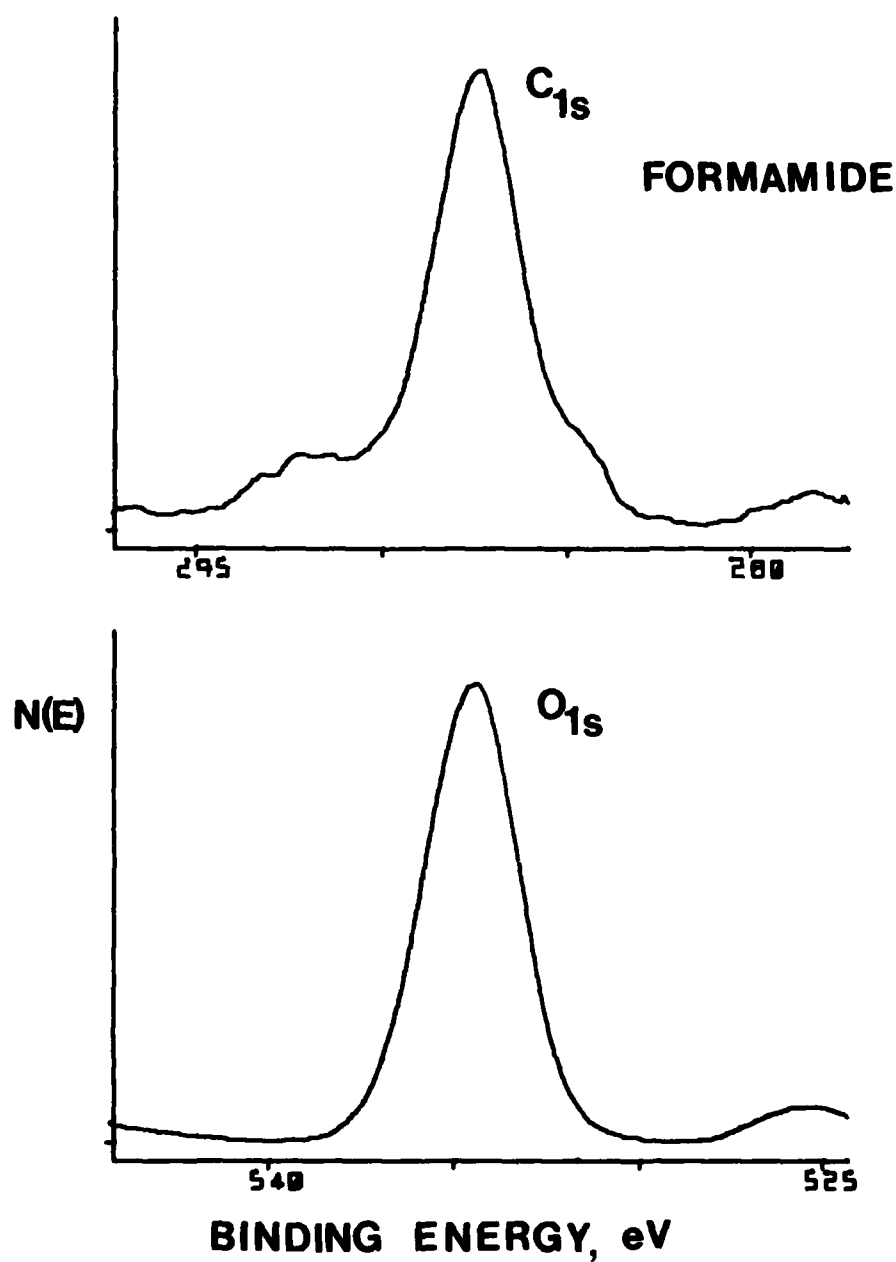


FIGURE 16 - C 1s and O 1s spectra of phosphoric acid anodized aluminum after 16 hr exposure to formamide and water vapors in air. Spectrometer pass energy was 65 eV.

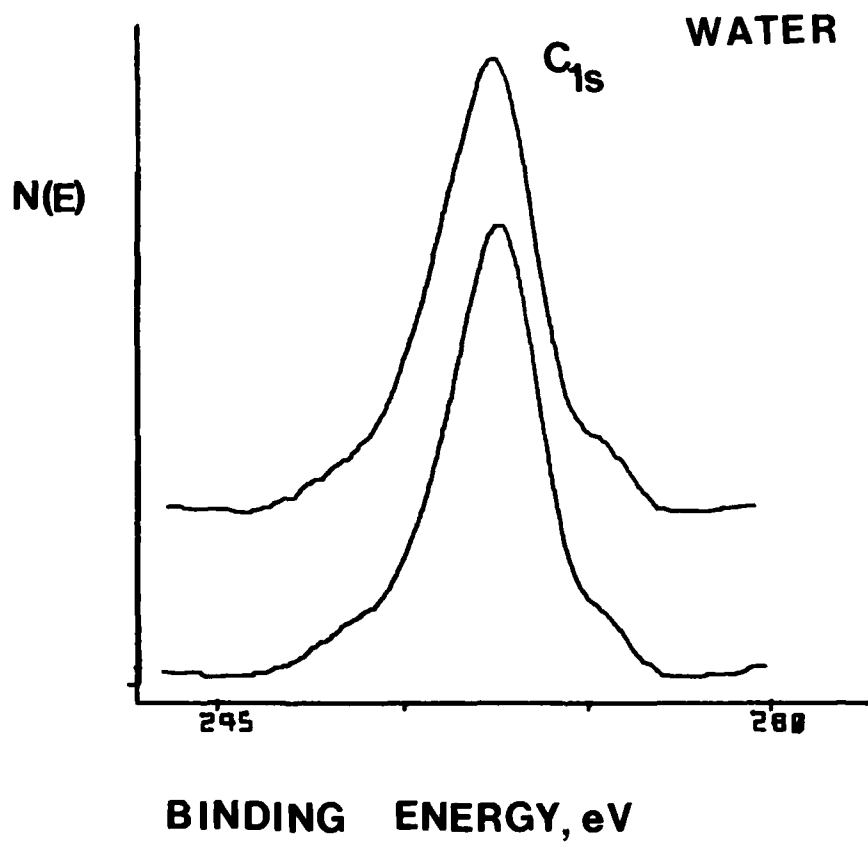


FIGURE 17 - C_{1s} spectra of phosphoric acid anodized aluminum (a) as prepared and (b) after 10 min exposure to water vapor in air. Spectrometer pass energy was eV.

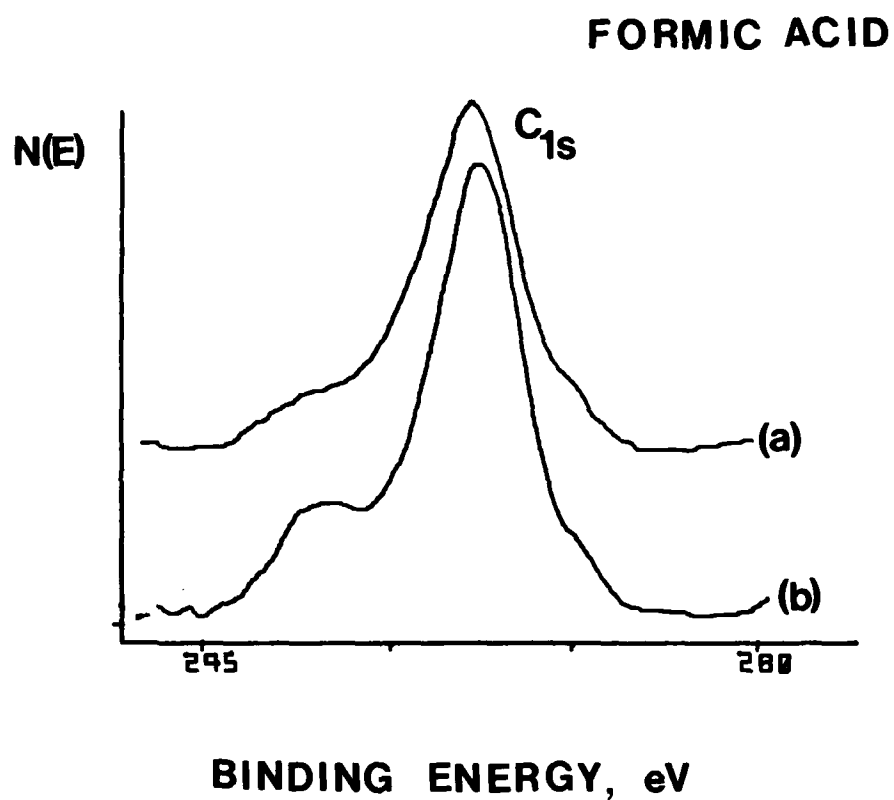


FIGURE 18 - C 1s spectra of phosphoric acid anodized aluminum (a) as prepared and (b) after 10 min to formic acid and water vapors in air. Spectrometer pass energy was 65 eV.

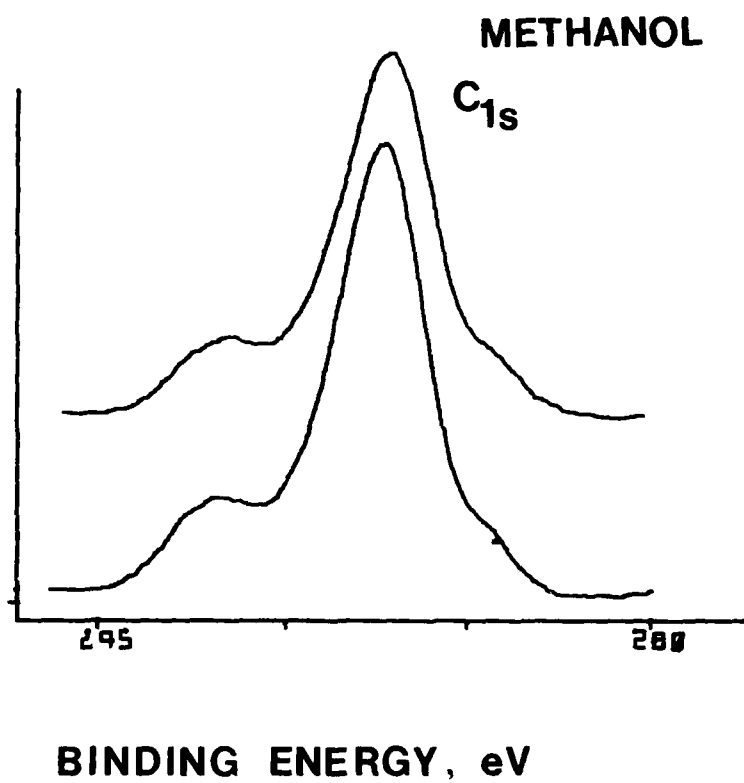


FIGURE 19 - C_{1s} spectra of phosphoric acid anodized aluminum (a) as prepared and (b) after 10 min exposure to methanol and water vapors in air. Spectrometer pass energy was 65 eV.

which did not adsorb on the anodized aluminum surface in vacuum (except for molecular adsorption achieved by freezing methanol onto a cooled surface, and which did not persist upon warming the sample back to room temperature), but which readily adsorbed onto the oxide in the presence of water vapor.

SECTION III

OTHER STUDIES RELATED TO ADHESIVE BONDING

1. SMUT ON STAINLESS STEEL SURFACES

Smut is a loosely adhering material that forms on materials such as Al, Ti, their alloys, and stainless steel during chemical treatment. Smut has been shown to decrease initial bondability and probably decreases effective service lifetime. It had been assumed by some workers that smut on their samples was due to graphite. The low carbon content and the availability of numerous known smutting materials including large amounts of Cu and Si, make it unlikely that smut on stainless steel consists only of graphite. AES and XPS measurements of smutted stainless steel surfaces showed the presence of Si and Cu on these surfaces in much larger amounts than on desmutted surfaces. The silicon found was in the form of silicon dioxide. From such studies of smut formation it may be possible to modify processes to eliminate it.

2. STRIPPABLE OXIDE FILMS

It is possible to use an anodization process that permits the oxide film to be stripped from a number of materials. This process may be of use in several technologies where fresh "super clean" surfaces are needed. On the other hand, such a surface is very undesirable for adhesive bonding, but it does serve as a model for interfacial failure to try to determine what bearing the chemistry at the interface has to do with adhesion. AES and XPS studies were made on Ta samples and F was found to be present on both the metal and oxide surfaces. Typical AES and XPS spectra from the stripped metal are shown in Figures 20 (a) and (b) respectively. It is planned to study specimens excluding or modifying F to determine the effect on adhesion.

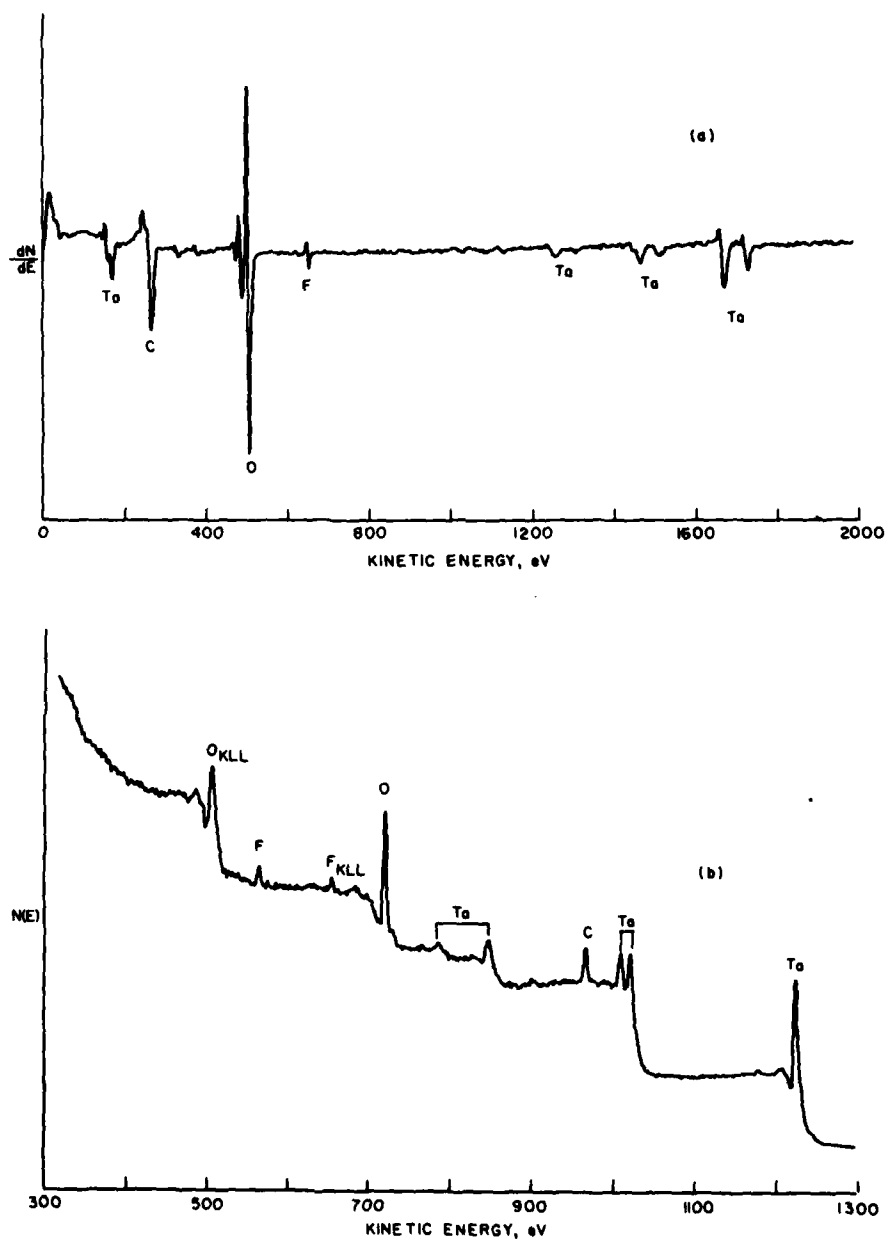


FIGURE 20 - Analysis of Ta after stripping its oxide, (a) using Auger electron spectroscopy, and (b) using X-ray photoelectron spectroscopy.

3. AES/XPS COMPARISON OF ACID TREATED ALLOYS

Quantative comparisons of the surfaces composition of 2024 and 7075 aluminum alloys following a sulfuric acid pickle were made. Auger spectra were analyzed using sensitivity factors from the "Handbook of Auger Electron Spectroscopy" whereas the XPS data were corrected for cross sections using Scofield's data.¹ XPS data were taken at 4 eV and 1 eV resolutions and peak heights and peak areas were used, respectively, in determining surface concentrations. The results from this study are listed in Table 1.

4. CORROSION STUDY OF PHOSPORIC ANODIZED ALUMINUM

One subject of interest in determining the durability of adhesively bonded joints is corrosion in the oxide layer. To examine this phenomena several samples of phosphoric acid anodized aluminum which had been subjected to corrosive atmospheres in an environmental test chamber were analyzed using the Scanning Auger Microprobe. Pitted areas were readily observable on these samples and AES spectra of the pits and surrounding areas were recorded. Typical spectra are presented in Figures 21 (a) and (b). This sample was 2024-T3 aluminum which had been exposed to a $\text{C Cl}_4 + \text{CH}_3\text{OH}$ environment for 30 minutes following anodization. The relative concentrations of chlorine and copper are seen to be much greater in the pitted area. Depth profiling using AES showed that the high concentration of copper persisted through the entire oxide layer. The presence of such pockets of copper from the bulk alloy in the oxide layer apparently are sites conducive to the beginning of corrosion of the surface.

5. XPS C 1s LINESHAPE STUDY ON AN ANODIZED ALUMINUM-ADHESIVE SYSTEM

An XPS carbon lineshape study was performed on an adhesive-adhered interface to look for chemical differences through the interface. Such studies should help clarify the amount of the chemical contribution to adhesive bonding. A sample consisting of a thin evaporated aluminum film which had been

TABLE 1
RELATIVE SURFACE CONCENTRATIONS OF ELEMENTS FROM A 7075
ALUMINUM ALLOY OBTAINED FROM AES AND XPS

ELEMENTS	RELATIVE CONCENTRATIONS		
	AES (PEAK-TO-PEAK HEIGHTS)	XPS (PEAK HEIGHTS)	XPS (PEAK AREAS)
Si	2.8	--	--
P	3.4	7.0	--
S	0.49	3.5	--
C	9.0	43	53
Ca	4.5	--	--
N	1.1	8.7	--
O	100	100	100
Cu	2.5	8.3	3.4
Zn	2.6	1.4	1.4
Mg	2.6	--	--
Al	68	43	55

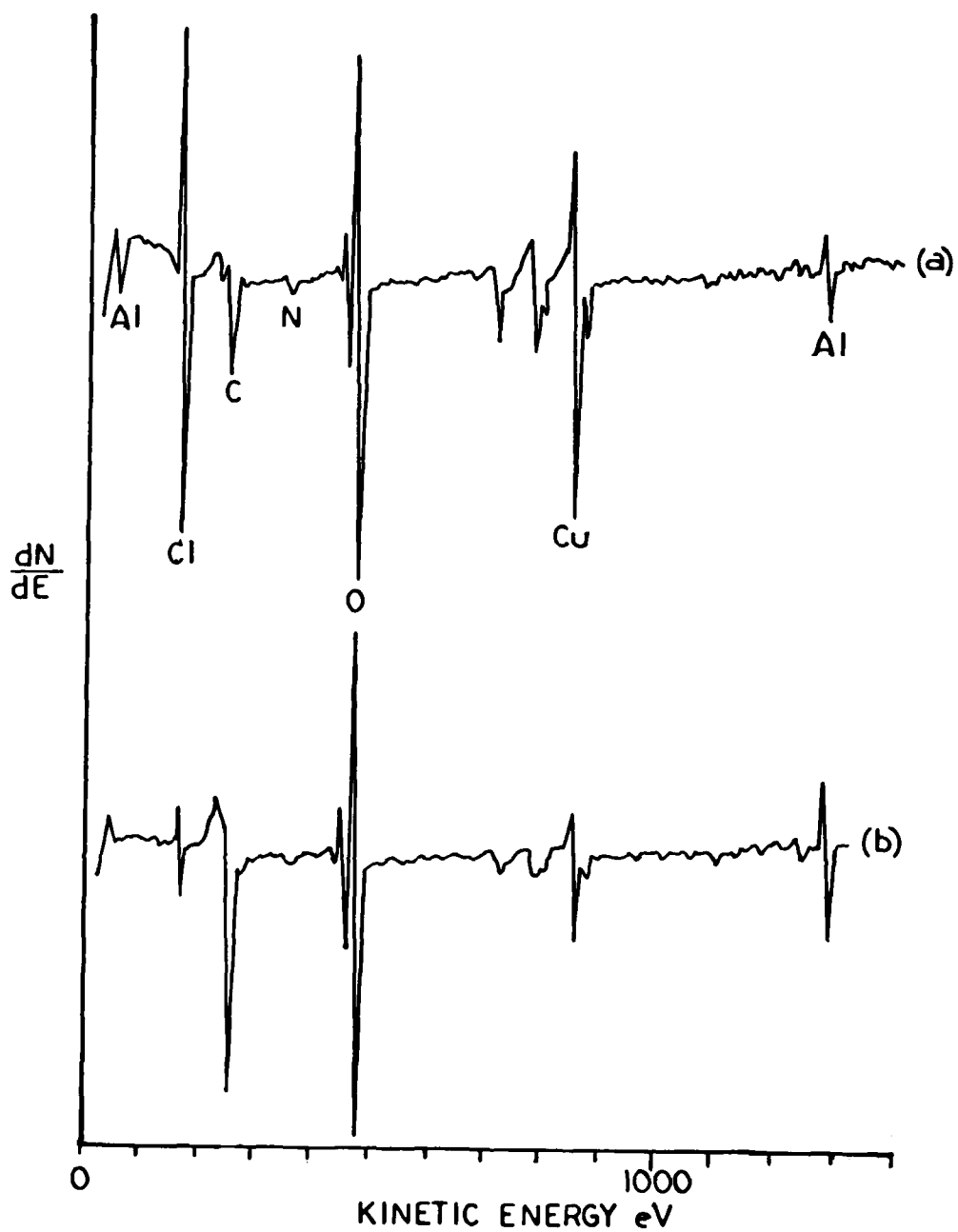


FIGURE 21 - AES spectra of anodized aluminum subjected to a corrosive atmosphere; (a) pitted area; (b) area near pit

anodized and then bonded to an aluminum substrate was analyzed. The sample was mounted so that the evaporated aluminum film could be ion etched away, to expose the oxide layer and then the adhesive. Auger spectra taken after sputtering into the oxide and adhesive are shown in Figure 22 (the offset of the spectrum from the adhesive is due to sample charging). High resolution (1 eV) XPS spectra of the carbon 1s line (shown in Figure 23) were then taken. There are obvious differences in the spectra, particularly the increases in a higher binding energy state of carbon in the adhesive.

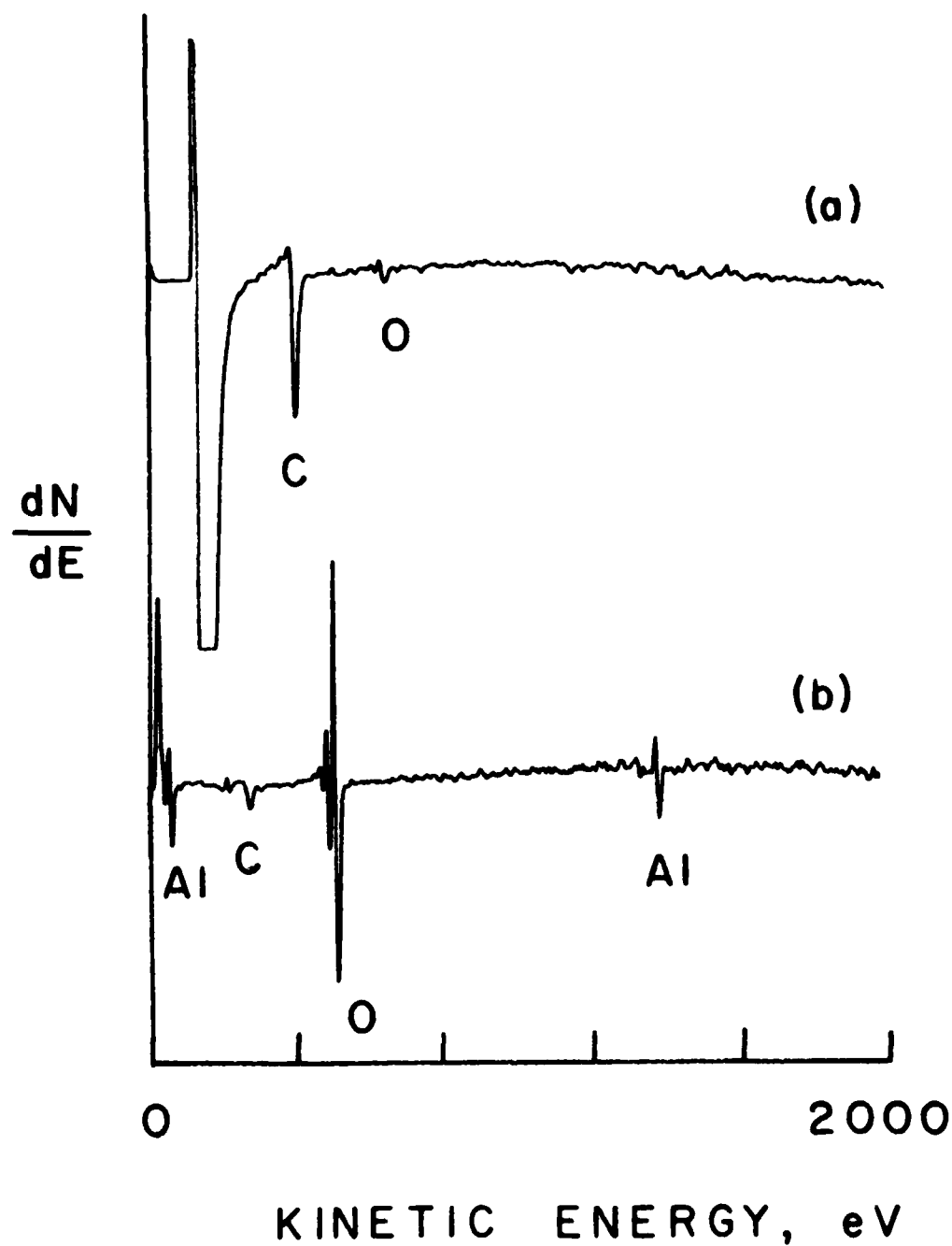


FIGURE 22 - AES spectra of Al_2O_3 adhesive sample (a) sputtered into adhesive and (b) sputtered into anodized layer. Modulation was 5 eV peak-to-peak.

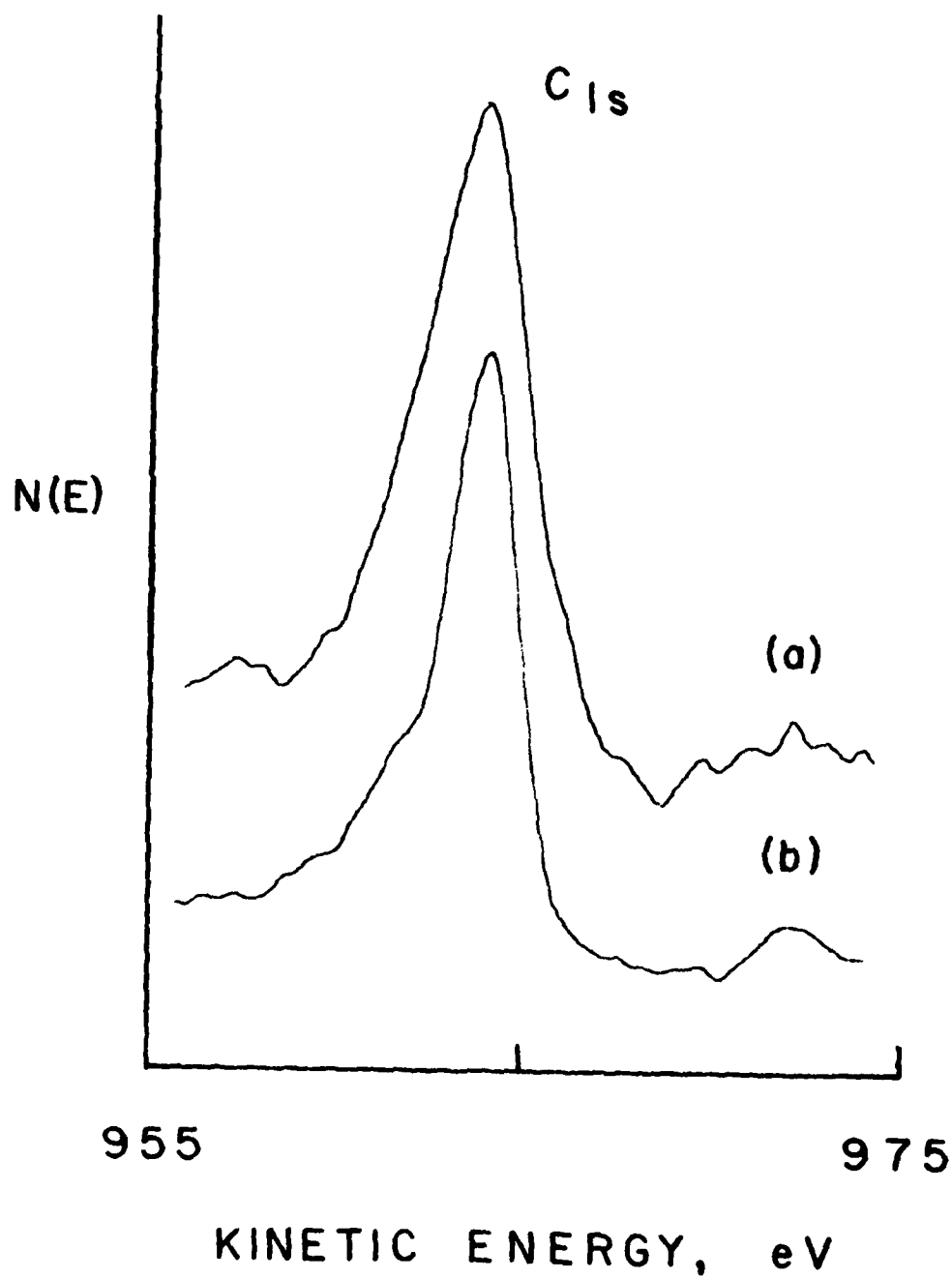


FIGURE 23 - Carbon 1s XPS spectra of $Al-Al_2O_3$ - adhesive sample (a) sputtered into adhesive layer and (b) sputtered into anodized layer. Spectrometer resolution was 1 eV.

SECTION IV

DECONVOLUTION OF XPS SPECTRA

In x-ray photoelectron spectroscopy x-rays emitted from an anode in the x-ray source strike the sample being analyzed, causing photoelectrons to be emitted from the energy levels within the sample. The energies of these electrons are then determined using a cylindrical mirror analyzer (CMA). The characteristics of the resultant spectrum are a combination of those of anode material, the sample, and the CMA. Therefore, a spectrum as recorded represents the energy levels within the sample, convoluted with the spectral distribution of the x-rays emitted from the anode, and this result convoluted with the response function of CMA. This convolution process produces a limitation on the information directly available from the spectrum, as it is the binding energies and line shapes and widths of the energy levels in the sample which are useful, and these are somewhat obscured by the spectral distribution of the x-ray source and the response of the analyzer.

Some of the obscured information can be recovered by deconvolution of the data, that is, mathematically processing the data so as to obtain an approximation of one of the components, in this case the energy levels of the sample. If we take F to represent these energy levels, A to represent the response function of the CMA, and I to be the energy distribution of the x-rays, the data, H , will be given by the expression.

$$H = F * A * I \quad (1)$$

where $*$ denotes the convolution operation. The convolution of two functions F and G is defined as

$$F * G = \int_{-\infty}^{+\infty} F(x-y) G(y) dy = \int_{-\infty}^{+\infty} F(y) G(x-y) dy. \quad (2)$$

Note that the operation has the property that

$$F * (G * H) = (F * G) * H = F * G * H \quad (3)$$

that is, it is associative.

We can take the total instrument response function, G , to be

$$G = A * I. \quad (4)$$

The problem then is given the recorded data, $H(E)$, to recover $F(E)$, where

$$H(E) = \int_{-\infty}^{+\infty} F(E-E') G(E') dE'. \quad (5)$$

If we can determine approximation to the source and analyzer response functions, and therefore $G(E)$, two iterative solutions for $F(E)$ can be found. They are

$$\begin{aligned} F_0(E) &= H(E) \\ F_{n+1} &= F_n + (H - F_n * G) \end{aligned} \quad (6)$$

and

$$\begin{aligned} F_0(E) &= H(E) \\ F_{n+1} &= F_n \cdot \frac{H}{(G * F_n)} \end{aligned} \quad (7)$$

where F_n is the n th approximation to $F(E)$, the approximation improving with increasing n .

In our calculations, the approach indicated in equation 7 has been used for two reasons. First, the negative values often produced in the other method cause the appearance of oscillations of the baseline in the vicinity of the peak. Secondly, it has been observed that the method of equation 7 produces a slightly greater degree of deconvolution for the same number of approximations.²

In our XPS studies, we have used a double-pass CMA in the retarding mode. This allows us to assume a response function of fixed energy width which is determined by the mirror voltage. Voltages corresponding to full

width at half maximum of 1 eV and 4 eV were used. The response of the analyzer was assumed to be gaussian with the appropriate width. The energy distribution of the incident radiation, the Mg K_{α} lines, was taken from the literature.³ The convolution of these two functions was calculated numerically, and the result was used as the instrument response function. The deconvolution calculation was then calculated numerically in a computer program (see appendix).

An initial test of this deconvolution method was performed by comparing a deconvoluted low resolution spectrum with a higher resolution spectrum of the same peaks. A spectrum of the calcium 2p doublet was recorded at 4 eV and at 1 eV resolution. These are shown in Figures 24 (a) and (d), respectively. An instrument response function representing only the broadening caused by the analyzer at 4 eV FWHM was then calculated and a total of 10 deconvolution approximations were made. The spectrum after 4 calculations is shown in Figure 24 (b). Here the separation of the $2p_{1/2}$ and $2p_{3/2}$ peaks is just appearing. The result after 10 calculations is shown in Figure 24 (c). Here we have achieved a resolution approximately the same as that in the spectrum taken at 1 eV resolution, Figure 24 (d).

A further test of this deconvolution method was made by resolving the C_{1s} doublet, which is not resolvable by the XPS system used in this work. A response function including the spectrometer response at 1 eV FWHM and the x-ray line shape for MgK_{α} radiation was used to deconvolute the spectrum shown in Figure 25 (a). The result after 5 approximations is shown in Figure 25 (b). Although the noise is considerably larger, the resolution of the $2p_{1/2}$ and $2p_{2/3}$ peaks is clear. Also note the attenuation of the higher-energy satellite peaks, which is due to the inclusion of the $MgK_{\alpha_{3,4}}$

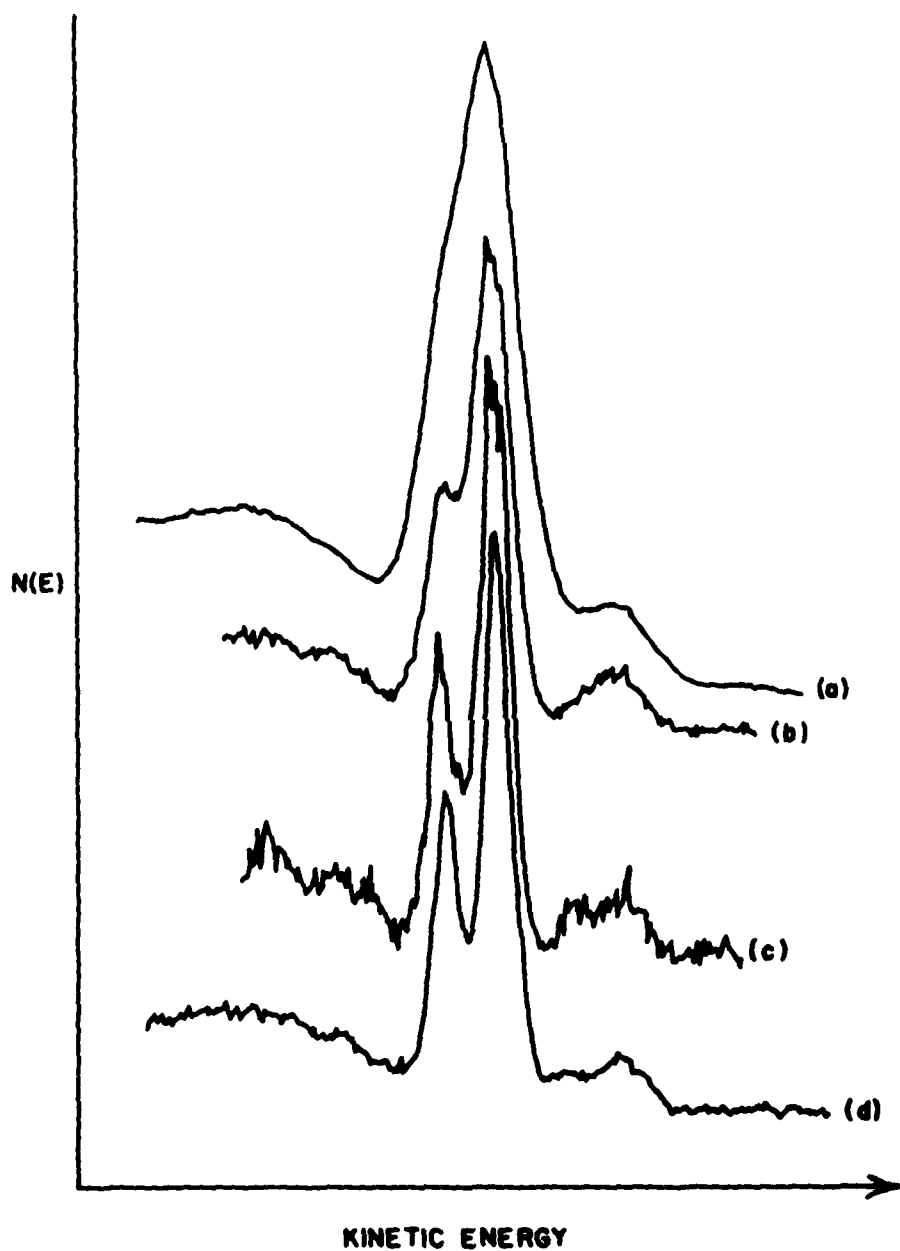


FIGURE 24 - Calcium 2p XPS spectra, (a) raw data with a spectrometer resolution of 4 eV, (b) after 4 deconvolution approximations, (c) after 10 deconvolution approximations, and (d) raw data with a spectrometer resolution of 1 eV.

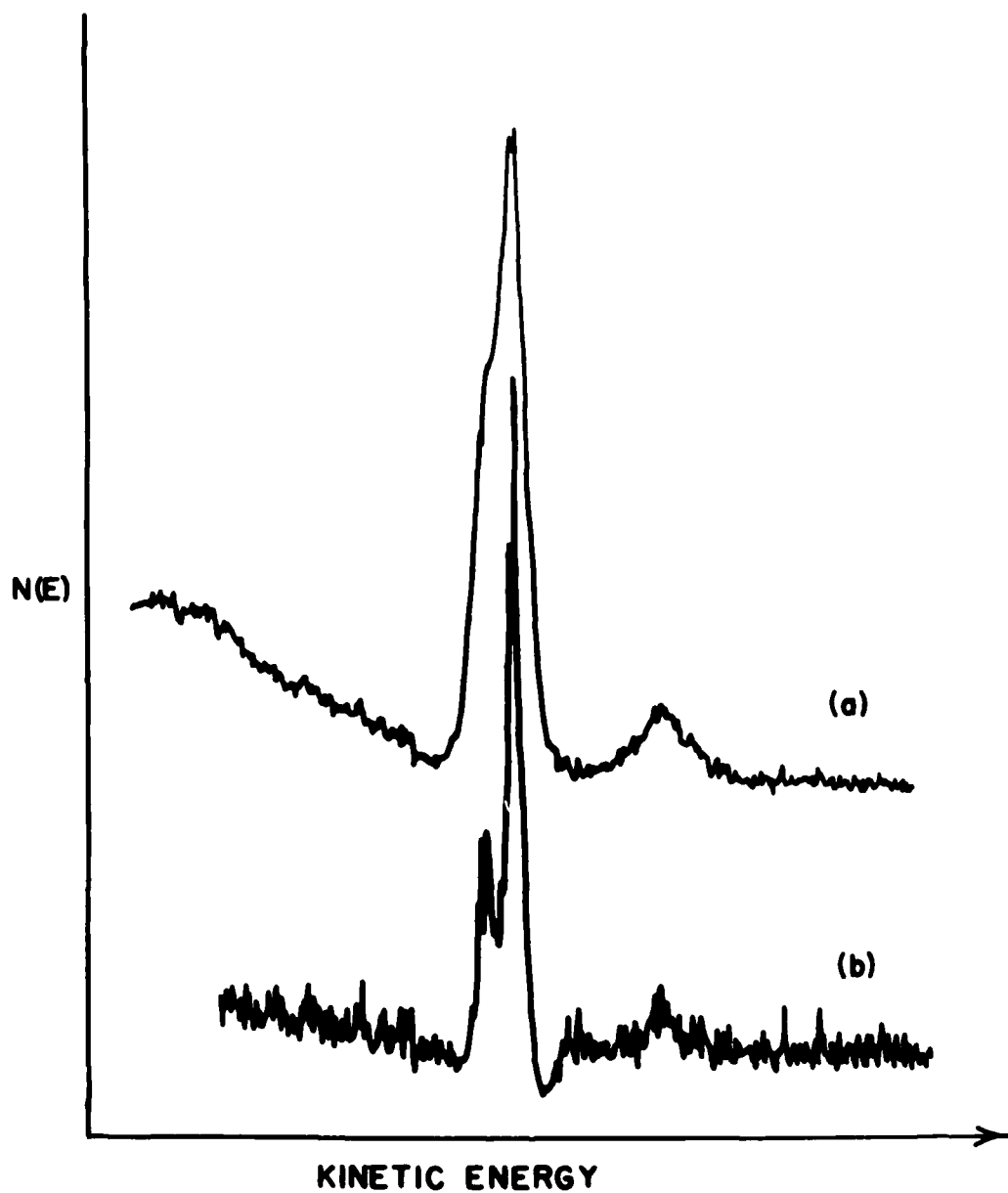


FIGURE 25 - Chlorine 2p XPS spectra, (a) raw data with a spectrometer resolution of 1 eV, and (b) after 5 deconvolution approximations.

lines, which produce these satellites, in the x-ray line shape function.

We can conclude that this deconvolution technique can be very useful in recovering information about the energy levels in the samples being analyzed which has been obscured due to instrumental broadening. We must note that, as in the examples above, the signal to noise is considerably reduced by the deconvolution process, so that it requires relatively noise-free spectra as a starting point.

SECTION V

GRAPHITE FIBERS

A number of graphite fibers have been studied during the course of the contract. These fibers were manufactured by Hercules and were prepared by coagulating acrylonitrile polymer in sodium sulfate and then graphitizing at 1500°C for AS and AU type fibers and about 2000°C for HMS and HMU type fibers. The AS and HMS fibers had been given the manufactures surface treatment (oxidation) whereas the AU and HMU fibers were untreated.

Initial XPS studies of these fibers as received were performed using $MgK\alpha$ radiation, including high resolution line shape studies as well as quantitative analysis of their elemental surface composition.

These studies were later repeated after the x-ray anode had been replaced with one which produced $AlK\alpha$ radiation. This was done to provide a basis for comparison for a study of fibers which had been heated in a vacuum. The vacuum heat treatment consisted of raising the temperature of the fibers in 50°C steps until a temperature of 300°C was achieved. The fibers were then kept at this temperature overnight. At 300°C and physisorbed species should be desorbed, however, there will be no change in the surface topography and chemisorbed species will remain. Also 300°C is the highest curing temperature for graphite fiber composites.

1. COMPARISON OF AS AND AU FIBERS USING $Mg K\alpha$ RADIATION

X-ray photoelectron spectroscopy (XPS) measurements showed that the surface compositions of these fibers were quite different from each other. Typical photoelectron spectra over a kinetic energy range from 100 eV to 1100 eV and shown in Figure 26. Clearly the surface concentrations of oxygen and nitrogen are higher on the AS fibers, Figure 26 (b), than on

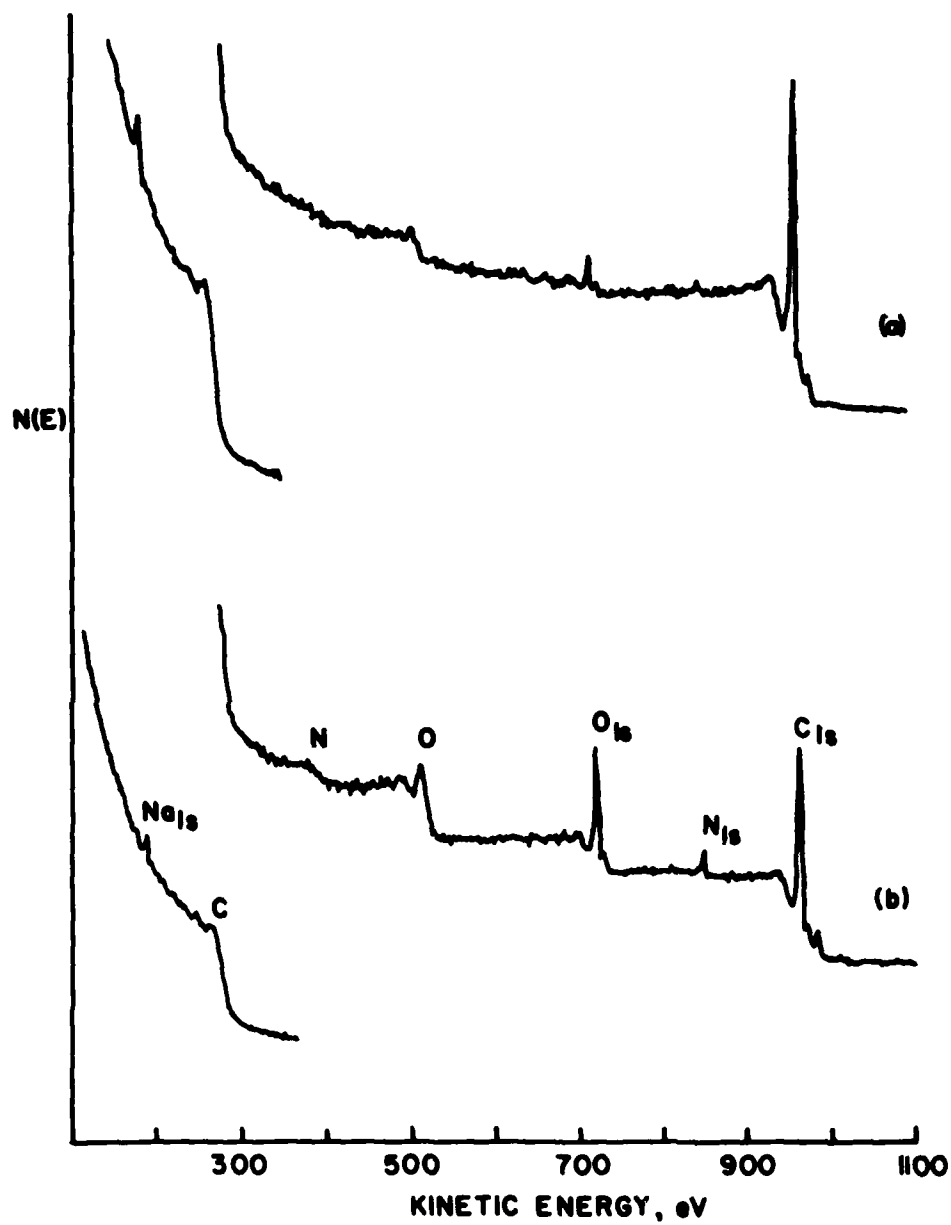


FIGURE 26 - XPS spectra of graphite fibers, (a) AU type fibers, and (b) AS type fibers. Spectrometer resolution was 4 eV.

the AU fibers, Figure 26 (a). Conversely, the surface concentration of sodium is lower on the AS fibers than on the AU fibers.

The larger oxygen concentration on the AS fibers is not unexpected as these fibers have been oxidized. The source of the nitrogen is not certain but its presence could indicate that the fibers were oxidized in nitric acid. The sodium contamination is probably due to coagulation in sodium sulfate.

The carbon, sodium oxygen, and nitrogen 1s photoelectron peak energies and full widths at half maximum (FWHM) were measured at a spectrometer resolution of 1 eV. The carbon, oxygen and sodium peak energies agreed within 1 eV for the four sets of fibers studied. The peak widths are listed in Table 2. There appeared to be a small carbon peak at about 4 eV higher binding energy than the main carbon peak on the AS fibers. The oxygen peak is wider than expected and may be comprised of more than a single peak. Higher resolution measurements are not feasible in our XPS system due to relatively low count rates. Measurements made on AS fibers using a new XPS system (PHI model 550), having a count rate estimated to be about 15X that used here, at about 0.3 eV spectrometer resolution showed a small improvement in resolution of the measured carbon 1s peak (1.9eV FWHM) and verified the existence of the small carbon peak at about 4 eV higher binding energy. (With the PHI model 550 at a spectrometer resolution of 0.3eV the measured FWHM of the silver $3d_{5/2}$ peak is 0.9 eV).

Calculations have been made of the surface concentrations of oxygen, nitrogen and sodium from the XPS data assuming that they are uniformly distributed throughout the surface region. Cross sections were taken from the data of Scofield¹, and the results are listed in Tables 3 and 4.

TABLE 2

MEASURED FULL WIDTHS AT HALF MAXIMUM (FWHM)
FOR C,O,Na AND N 1s PHOTOELECTRON PEAKS FROM
AS AND AU FIBERS

FWHM		
<u>Peak</u>	<u>AS Fiber</u>	<u>AU Fiber</u>
C	2.25	2.25
O	3.25	3.25
Na	2.25	2.25
N	2.75	--

TABLE 3

CONCENTRATION IN ATOMIC PER CENT IN GRAPHITE FIBERS:
CALCULATED FROM 1s PEAK HEIGHTS UNDER 4eV RESOLUTION

	<u>C</u>	<u>O</u>	<u>N</u>	<u>Na</u>
AU ₁	88	6.1	-	5.3
AU ₂	91	2.7	1	5.3
AS ₃	79	15	3	2.8
AS ₄	77	15	5.4	2.4
HMU ₁	97	2.5	-	-
HMU ₂	97	3.1	-	-
HMS ₁	94	5.5	-	-
HMS ₂	95	4.9	-	-

TABLE 4

CONCENTRATIONS IN ATOMIC PER CENT IN GRAPHITE FIBERS:
CALCULATED FROM 1s PEAK AREAS UNDER 1 eV RESOLUTION -

	<u>C</u>	<u>O</u>	<u>N</u>	<u>Na</u>
AU ₂	92	5.5	-	4.0
AS ₄	73	19	5.5	2.4
HMU ₂	90	10	-	-
HMS ₂	87	13	-	-

It can be seen from these tables that the sodium concentration for the AU type fibers is about twice that for the AS type fibers. As the sodium 2s XPS peaks can also be measured, a check can be made of the uniformity of the sodium distribution throughout the surface layer as the 2s photoelectrons have a kinetic energy of about 1190 eV, compared with about 180 eV for the sodium 1s photoelectrons, and therefore a longer escape depth. (The 2s photoelectrons would have an escape depth about $2\frac{1}{2} \times$ that of the 1s photoelectrons). For a uniform sodium distribution, the ratio of the 1s to 2s peaks should be constant. Measurements on two sets of AU type fibers yielded signal ratios (peak areas not corrected for cross sections or instruments resolution) of 4.17 and 3.72, whereas for AS fibers ratios of 2.04 and 1.84 were obtained. Therefore, it appears that there is a higher concentration of sodium nearer the surface for the AU fibers compared with the AS fibers.

2. COMPARISON OF HMS AND HMU FIBERS USING Mg K $_{\alpha}$ RADIATION

XPS measurements showed that the surface compositions of these fibers were different from each other and from the AS and AU type fibers, Figure 27.

No sodium was detected from the HMS or HMU fibers. As mentioned earlier these fibers were graphitized at a higher temperature than the AS and AU fibers (about 2000°C) so no sodium contamination was expected.

The surface treated fibers, HMS, also showed a larger concentration of oxygen than the untreated fibers, HMU - see Tables 3 and 4.

The carbon and oxygen 1s photoelectron peak energies and full widths at half maximum were also measured at a spectrometer resolution of 1 eV. The carbon and oxygen peak energies from the different fibers were within 0.2 eV for carbon and 0.5 eV for oxygen. The FWHM for carbon and oxygen

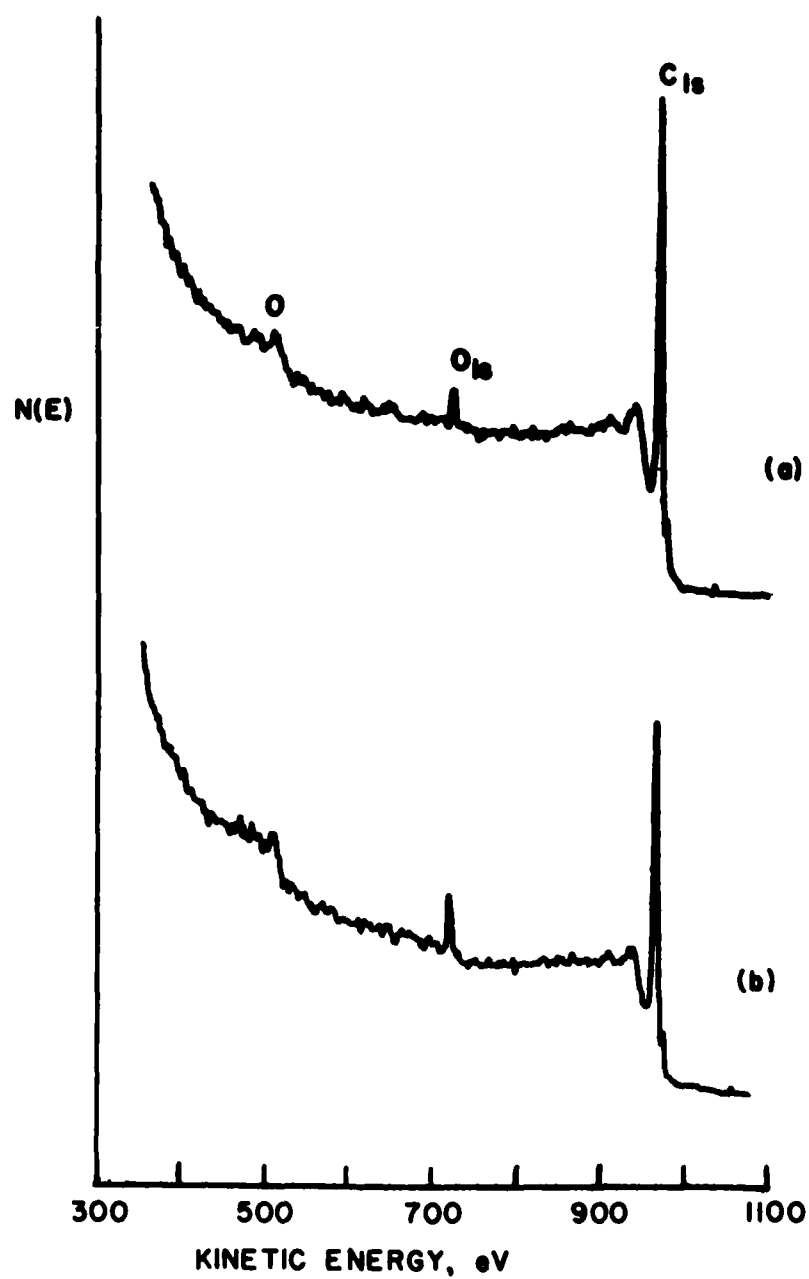


FIGURE 27 - XPS spectra of graphite fibers, (a) HMU type fibers, and (b) HMS type fibers. Spectrometer resolution was 4 eV.

were measured to be 1.6 eV and 3.4 eV respectively. The FWHM for oxygen is similar to that from the AS and AU fibers, but the FWHM for carbon is considerably narrower than that from the AS and AU fibers (1.6 eV compared to 2.25 eV), Figure 28. This result is not unreasonable as the higher graphitization temperature for the HMS and HMU fibers should in more truly graphitic surfaces.

3. EFFECT OF VACUUM HEAT TREATMENT ON FIBERS

After an AlK α x-ray source was mounted on the spectrometer samples were prepared to study the effects of vacuum heat treating the samples. Two new samples of the AS, AU, HMS and HMU fibers each were prepared. One of each type of fiber were mounted in a vacuum chamber (base pressure 5×10^{-6} Pa), heated to 300°C, and kept at that temperature overnight. As this treatment was performed in another vacuum chamber and the samples had to be transferred through air only irreversible changes in the fiber surfaces were detected.

XPS measurements of the fiber surfaces before and after the vacuum heat treatment are presented in Figures 29, 30, 31, and 32. Quantitative calculations of elemental surface concentrations were made by measuring the areas under the peaks from high resolution spectra and correcting for elemental sensitivities using published theoretical cross-sections for photoionization. These concentrations are listed in Table 5.

There is very good agreement between the surface concentrations for the fibers as received as calculated from the AlK α and MgK α excited spectra. It should be remembered that the aluminum x-ray energy is 232 eV higher than that of the magnesium, so that the escape depths of the electrons excited by the aluminum anode will be greater. Therefore the

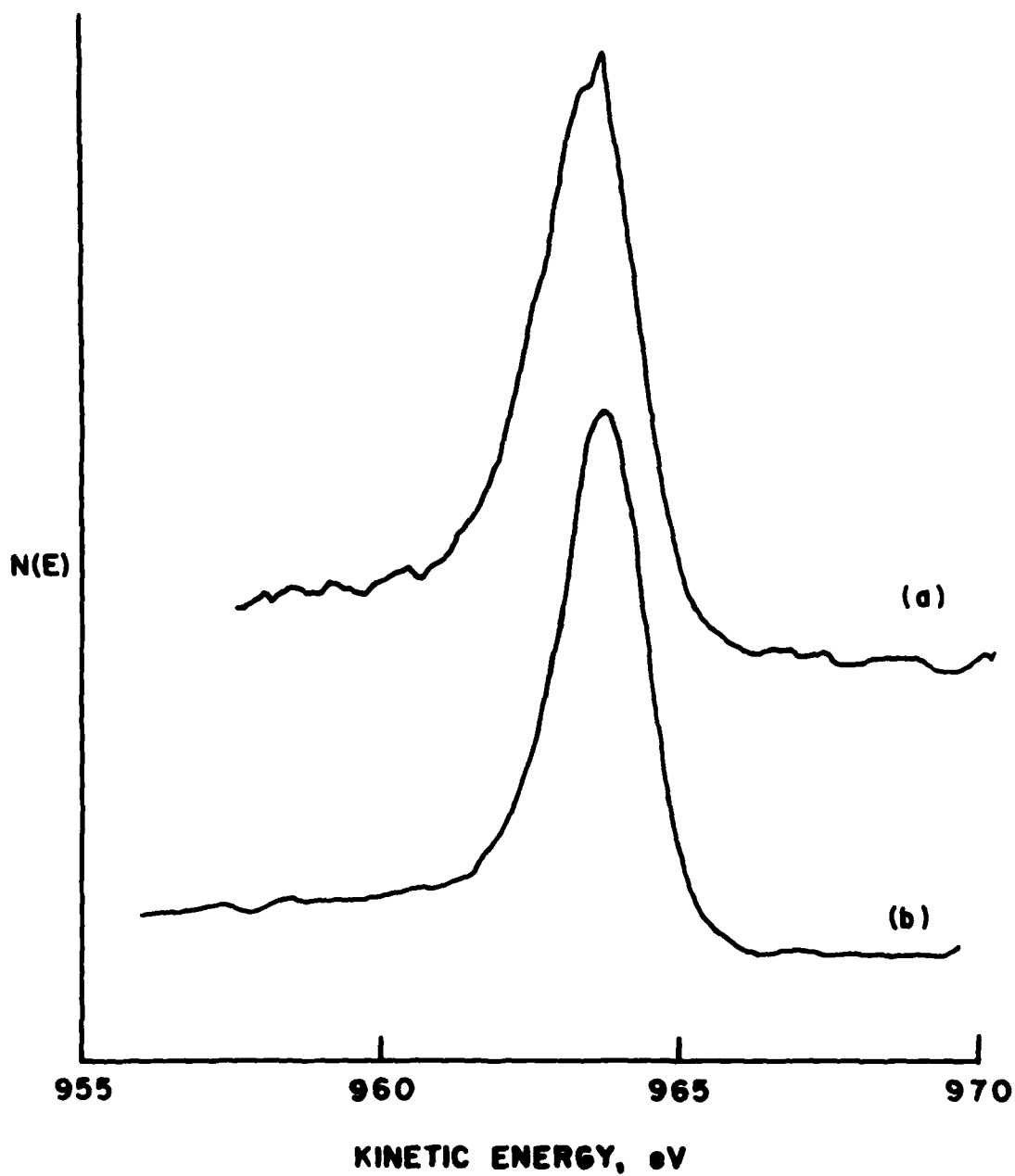


FIGURE 28 - Carbon 1s XPS spectra from, (a) AS type fibers, and (b) from HMU type fibers. Spectrometer resolution was 1 eV.

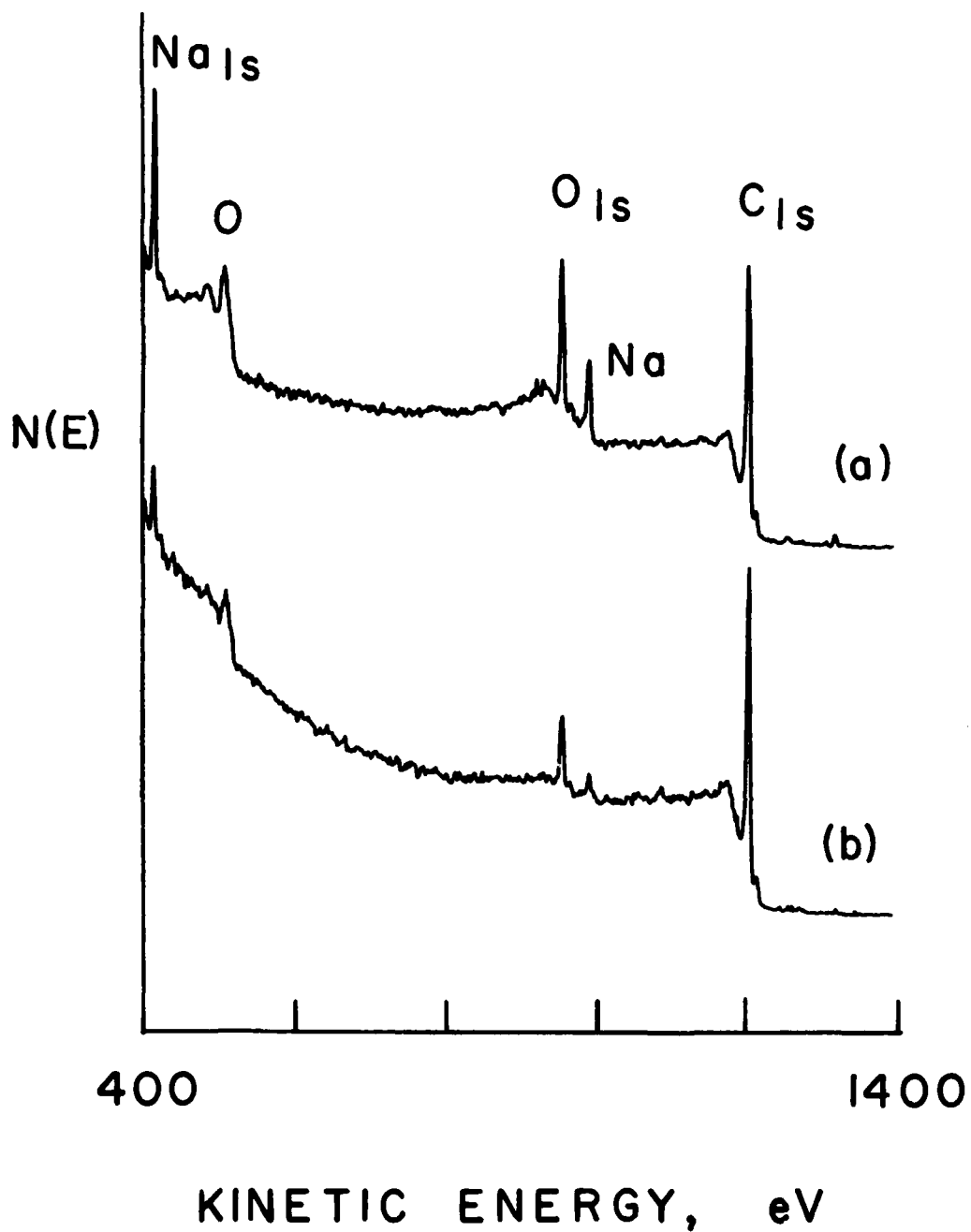


FIGURE 29 - XPS spectra of AU type graphite fibers (a) after 300° vacuum heat treatment and (b) as received. Spectrometer resolution was 4 eV.

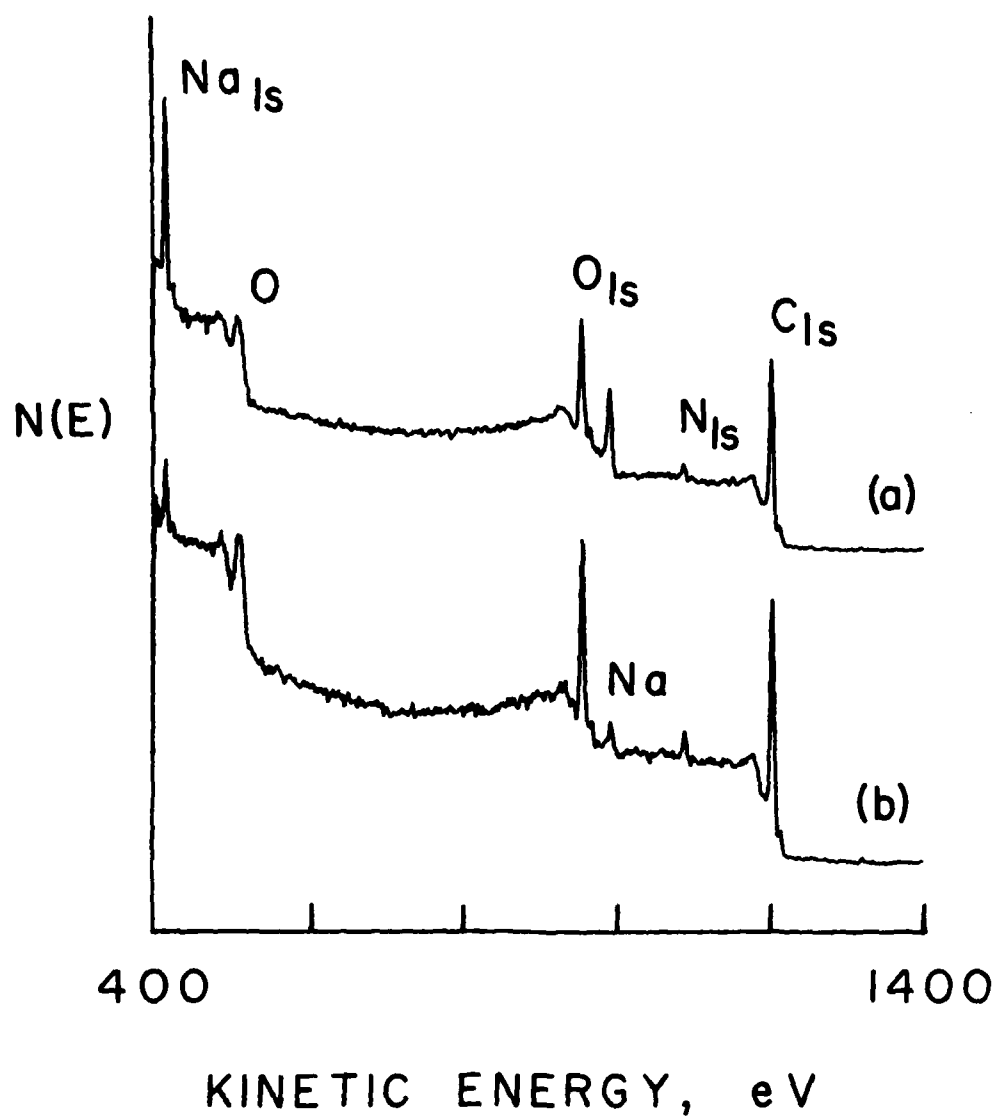


FIGURE 30 - XPS spectra of AS type graphite fibers (a) after 300°C vacuum heat treatment and (b) as received. Spectrometer resolution was 4 eV.

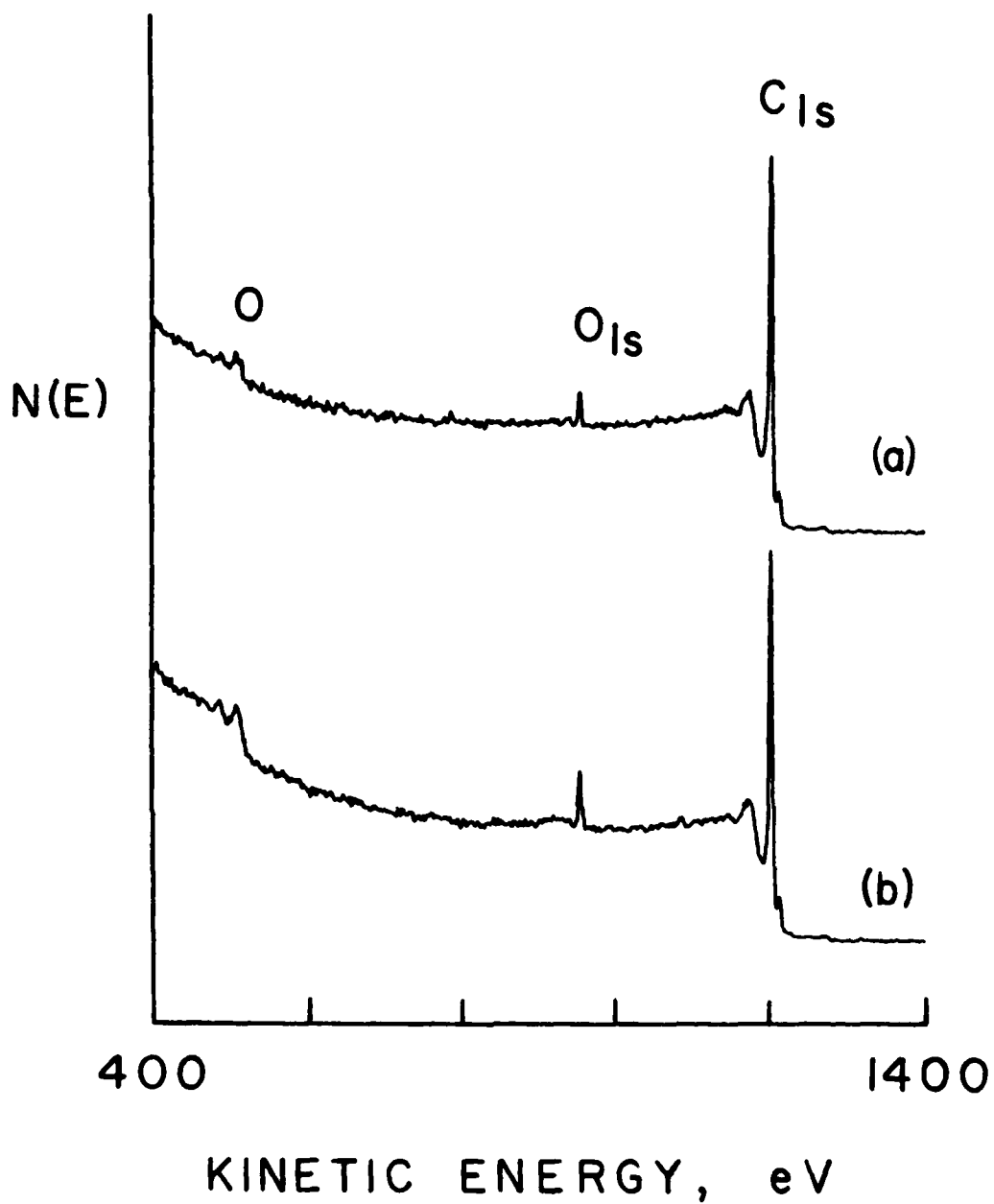


FIGURE 31 - XPS spectra of HMU type graphite fibers (a) after 300° vacuum heat treatment and (b) as received. Spectrometer resolution was 4 eV.

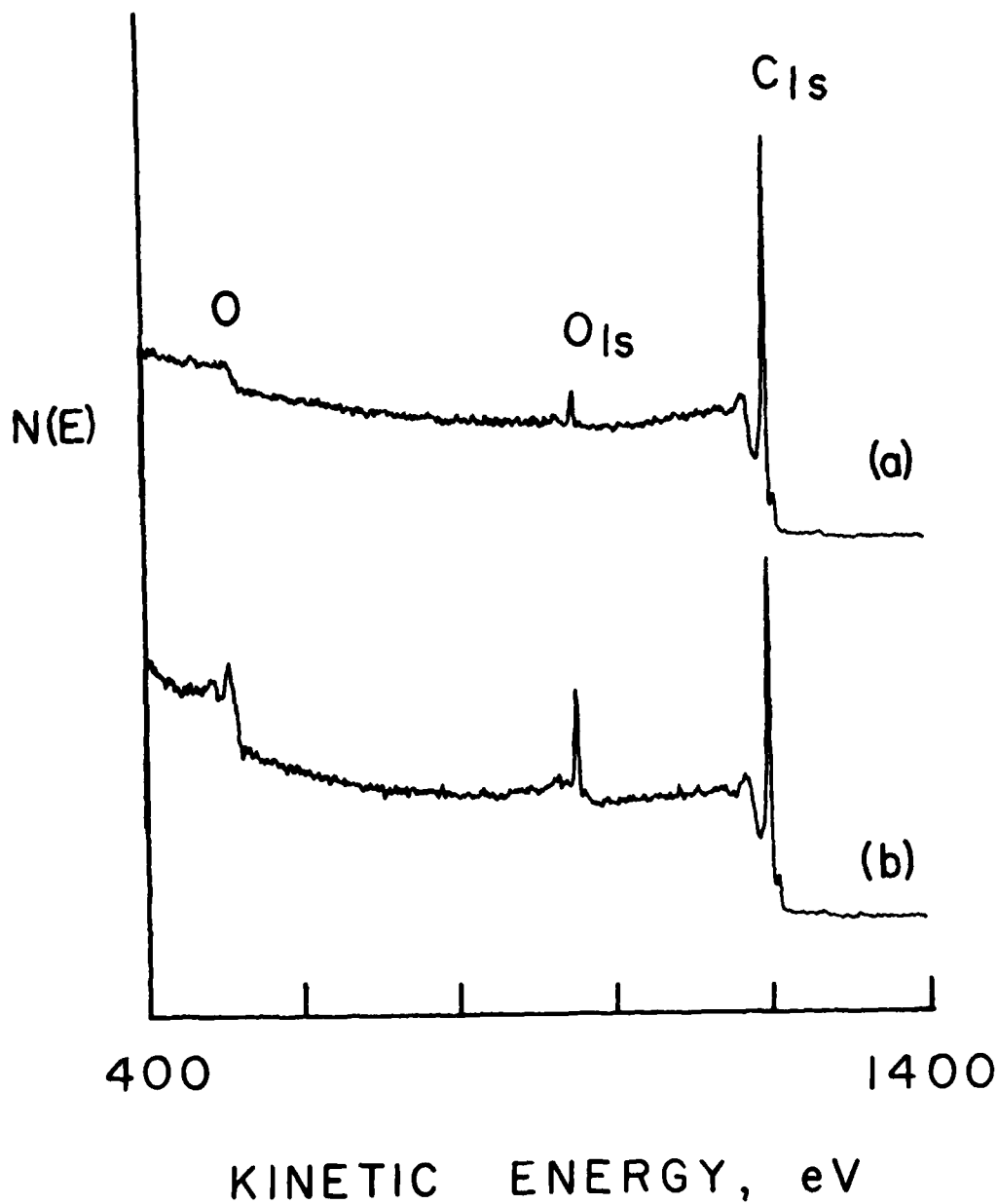


FIGURE 32 - XPS spectra of HMS type graphite fibers (a) after 300° C vacuum heat treatment and (b) as received. Spectrometer resolution was 4 eV.

TABLE 5

CONCENTRATIONS IN ATOMIC PER CENT IN GRAPHITE FIBERS:
CALCULATED FROM 1s PEAK AREAS UNDER 2eV RESOLUTION

	<u>C</u>	<u>O</u>	<u>Na</u>	<u>N</u>	<u>S</u>
AUR	86	9	3	2	-
AUV	79	14	6	*	2
ASR	70	20	4	7	*
ASV	72	18	6	3	-
HMUR	95	5	-	*	-
HMOV	96	4	-	-	-
HMSR	89	9	-	1	-
HMSV	97	3	-	-	-

* Below measurable limit

thickness of the layer which we are sampling has increased, and some differences may be expected.

In all the samples the heat treatment has produced a depletion in the nitrogen. Also, traces of sulfur were detected on the AU and AS fibers, probably from the sodium sulfate used in producing the fibers. The substantial increase in the sodium on the surfaces of the A type fibers is brought about by driving the sodium in the bulk of the fibers to the surface upon heating. There is an increase in oxygen concentration on the AU fiber following heating, whereas the other three fibers show a slight decrease in the oxygen content.

Figures 33 and 34 show scans of the carbon and oxygen 1s peaks from the AS fibers taken at 2 eV resolution before and after the heat treatment. As discussed in the MgK α excited spectra, the shoulder to the lower kinetic energy side of the carbon 1s peak in as received condition represents a second (higher binding energy) chemical state. Inspection of the spectra taken after the heat treatment shows that this shoulder is no longer present, indicating a reduction of this carbon, and the appearance of a low kinetic energy shoulder in the oxygen 1s peak (Figure 34) shows that corresponding formation of a high binding energy oxygen state has occurred.

A further investigation of the effects of vacuum heat treatment on the AS fiber was performed. Two more samples were prepared, the first having been heated to 600°C until the outgassing products stabilized, the second was heated to 700°C for one hour and then reduced in H₂ for an hour. These samples are denoted as ASV6 and AS7H, respectively. Atomic concentrations were calculated from XPS peak areas as described previously, the results being given in Table 6.

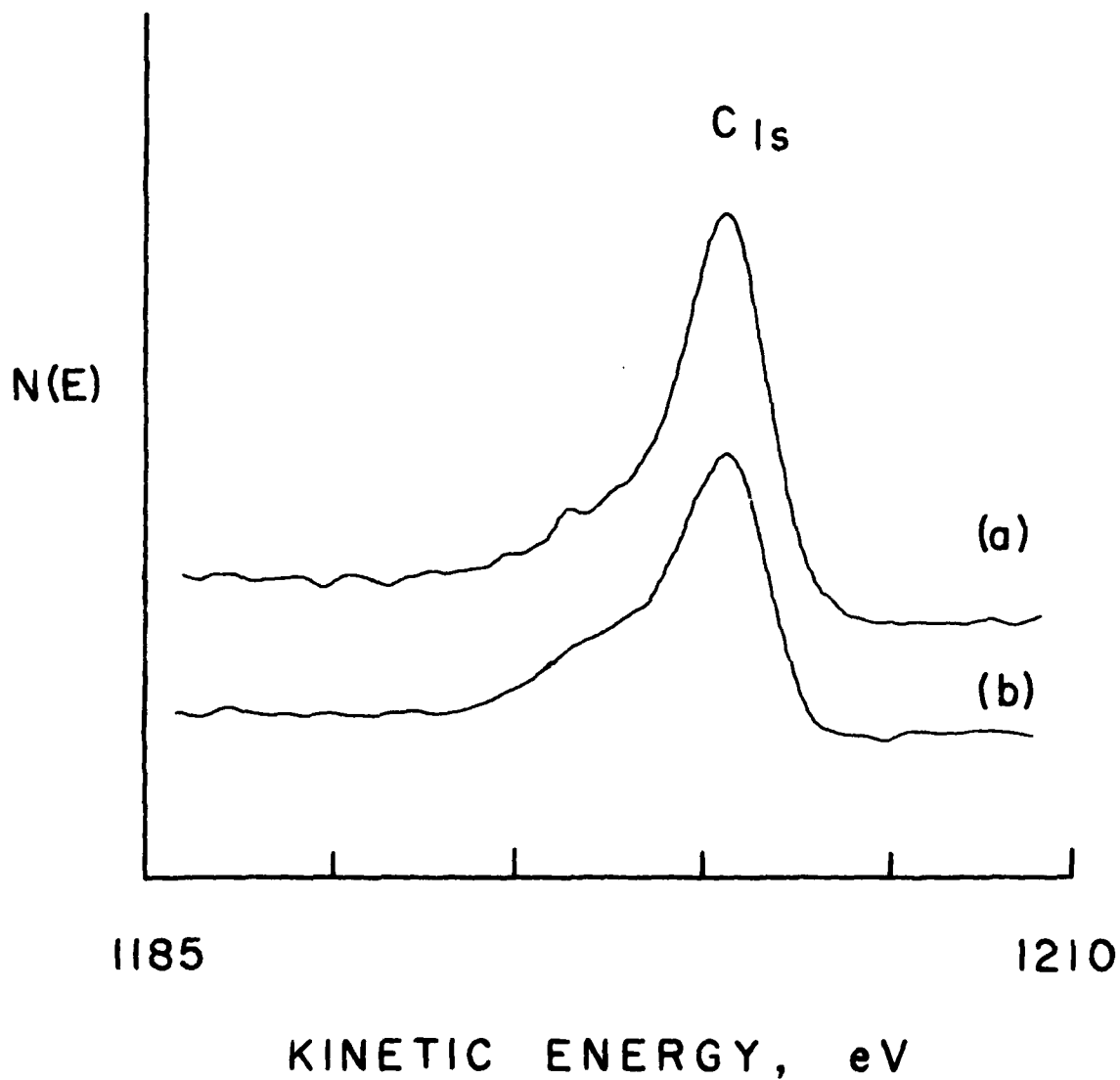


FIGURE 33 - Carbon 1s XPS spectra of AS fiber (a) after 300°C vacuum heat treatment and (b) as received. Spectrometer resolution was 2 eV.

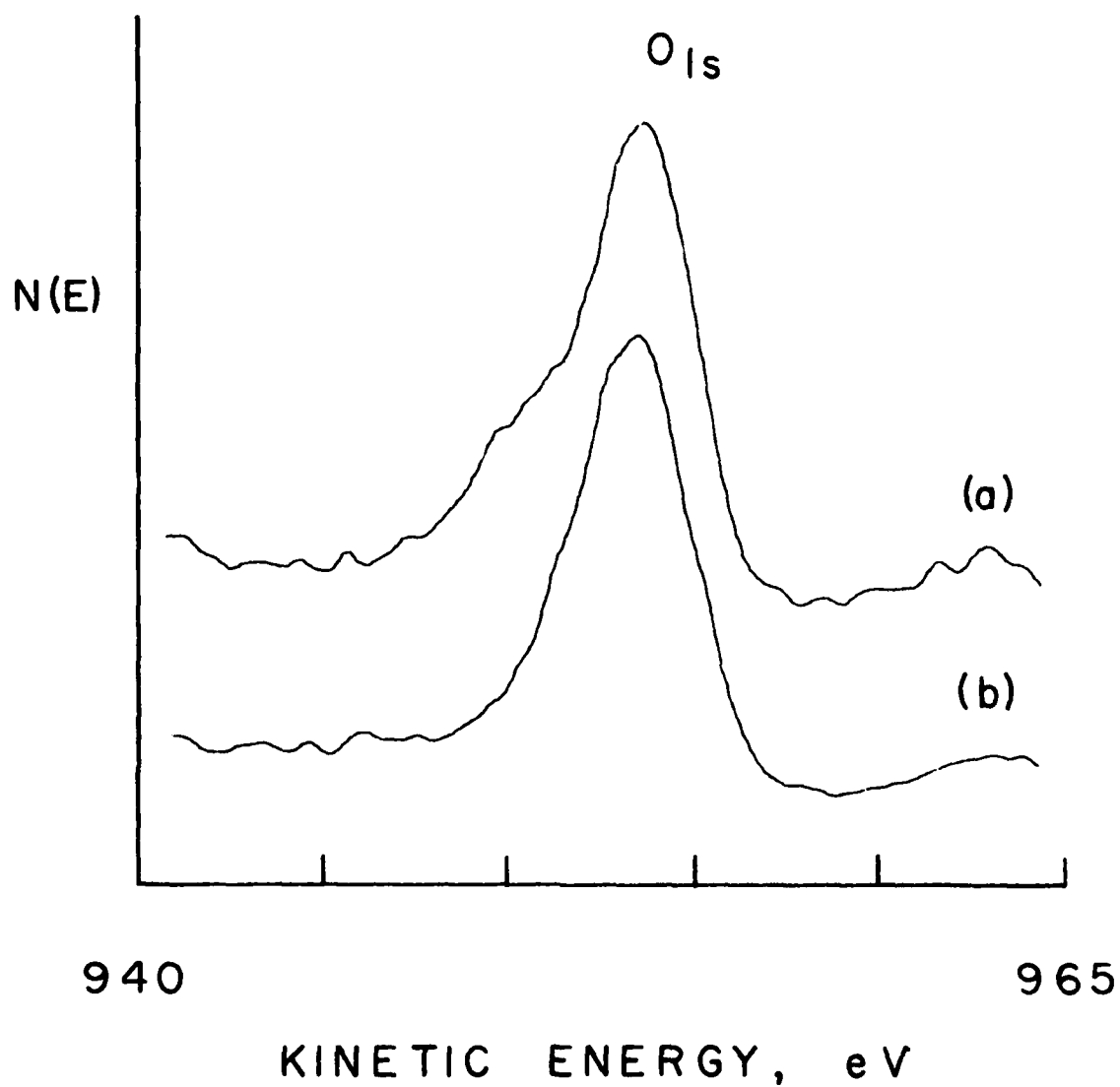


FIGURE 34 - Oxygen 1s spectra of AS fiber (a) after 300°C vacuum heat treatment and (b) as received. Spectrometer resolution was 2 eV.

TABLE 6

CONCENTRATIONS IN ATOMIC PER CENT IN GRAPHITE FIBERS:
CALCULATED FROM 1s PEAK AREAS UNDER 2eV RESOLUTION

	<u>C</u>	<u>O</u>	<u>Na</u>	<u>N</u>	<u>S</u>
ASR	70	20	4	7	*
ASV	72	18	6	3	-
ASV6	84	7	6	3	1
AS7H	94	3	1	1	1

* Below measurable limit

The nitrogen, oxygen, and sodium concentrations decreased with higher temperatures, whereas a slight increase in sulfur was observed. Note that the composition of the AS7H fiber is similar to that of the untreated HM type fiber (Table 5).

High resolution (1eV) spectra of the carbon 1s peak on these fibers are shown in Figure 35. It is apparent that the high temperature heat treatments have produced a narrowing of the carbon lineshape, causing it to approach that of the sharp α graphitic line measured from the HMU fiber. Therefore both the chemical state of the AS fiber become similar to those of the HMU fiber as a result of higher temperature vacuum heat treatment.

4. FOREIGN MADE FIBERS

A set of foreign made fibers was characterized using Auger electron spectroscopy (AES). Boron, nitrogen, carbon, and a small amount of oxygen were detected, Figure 36. The boron and nitrogen Auger line shape and relative signal strengths indicated the presence of boron nitride (by comparison with a standard spectrum of boron nitride). The boron nitride layer was estimated as approximately 10 nm thick (based on Ta_2O_5 sputtering rate).

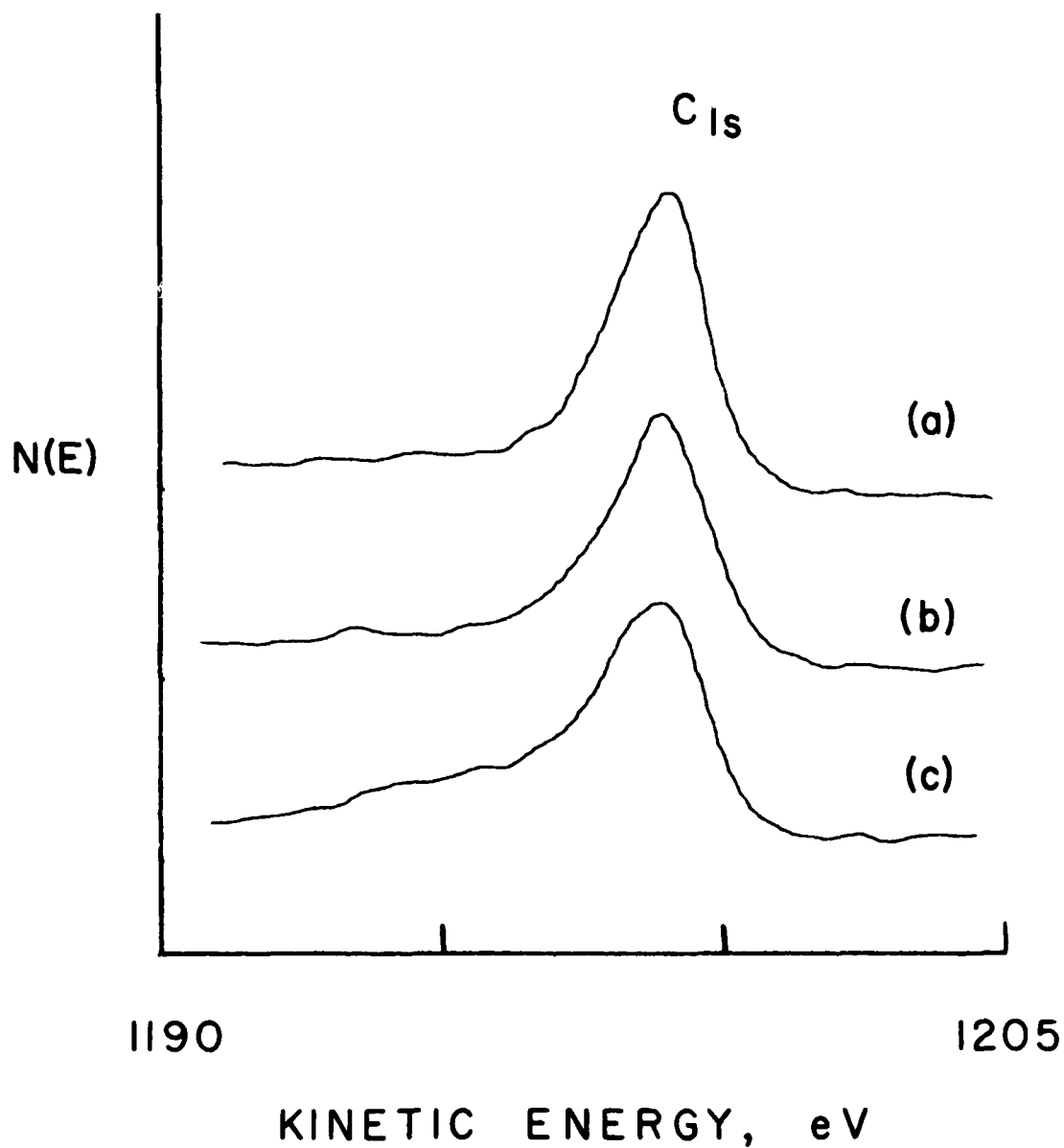


FIGURE 35 - Carbon 1s XPS spectra from (a) AS7H, (b) ASV6, and (c) As graphite fibers. Spectrometer resolution was 2 eV.

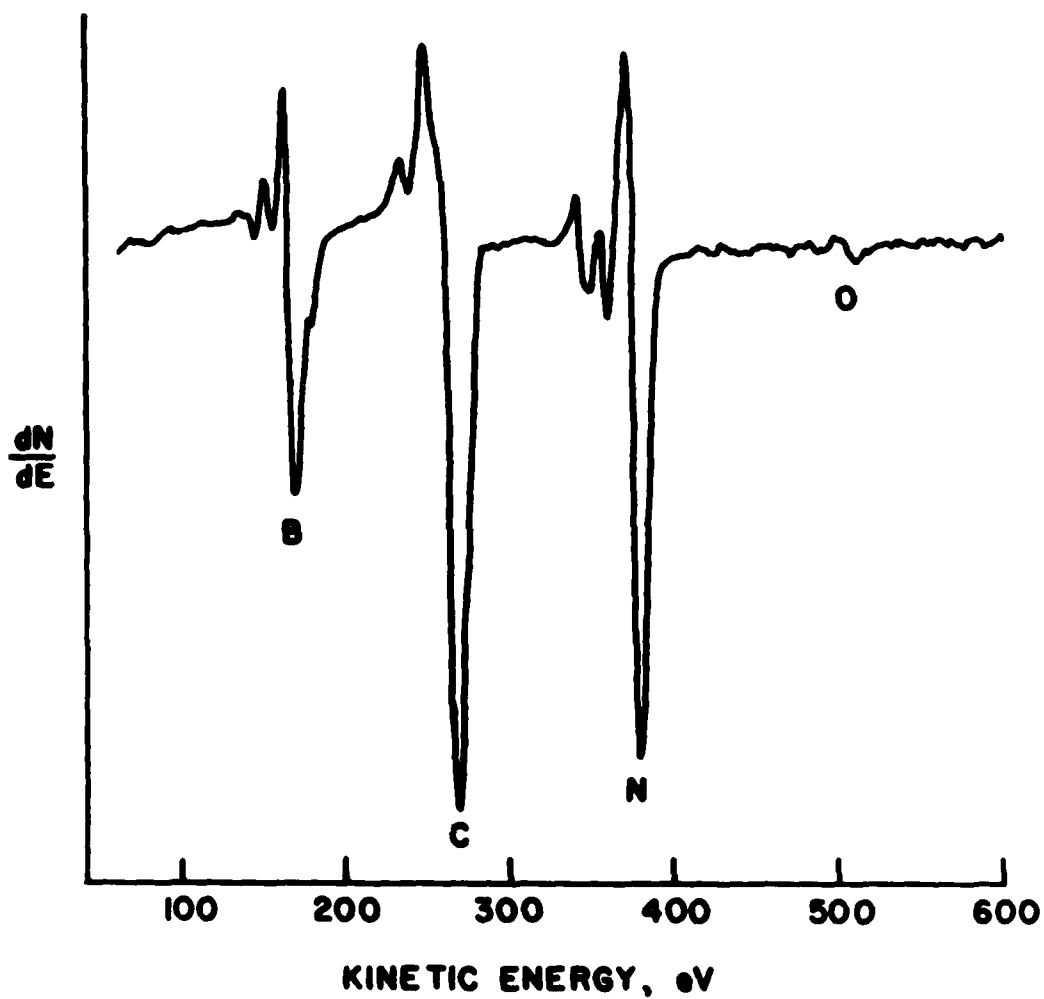


FIGURE 36 - Auger electron spectrum from foreign made fibers.
Electron beam energy was 3 keV, time constant 0.3s
and modulation (sinusoidal) 6 eV peak-to-peak.

SECTION VI

SOLID LUBRICANT FILMS

Molybdenum disulfide is often used as a solid lubricant film but little is known about changes in chemistry of the film surface that occur during wear. Two partly worn gas bearings were characterized here using mainly XPS. The lubricant film consisted of a mixture of co-sputtered molybdenum disulfide MoS_2 and antimony oxide Sb_2O_3 .

AES and XPS survey scans from one of the specimens are shown in Figure 37. The AES spectrum, Figure 37 (a), shows the presence of Mo, S, Sb, O (and C). The XPS spectrum, Figure 37 (b), also shows the presence of Mo, S, Sb, O (and C) peak. This overlap problem was verified by comparing high resolution XPS data from a $\text{MoS}_2 + \text{Sb}_2\text{O}_3$ burnished film with XPS data from partly oxidized Sb from InSb. These high resolution XPS spectra are shown in Figure 38 (a) and 38 (b) respectively. In Figure 38 (b) two sets of antimony 3d peaks are seen, the more intense pair being from Sb bonded in InSb and the weaker pair being from oxidized Sb. The energies of this latter pair of peaks agree well with those obtained from the burnished film, Figure 38 (a). The ratio of the antimony $3d_{5/2}$ to $3d_{3/2}$ peaks was measured to be 1.4 in the oxygen free state whereas it was about 1.8 in the oxidized state and in the burnished film. Obviously the increase in this ratio is due to the overlap of the oxygen 1s peak with the oxidized antimony $3d_{5/2}$ peak.

Useful information about the oxidation of molybdenum sulfide has also been obtained using XPS. Molybdenum 3d spectra from two partly worn gas bearings are shown in Figure 39. Like antimony, the molybdenum 3d spectrum is doublet so different molybdenum chemical states (at least two)

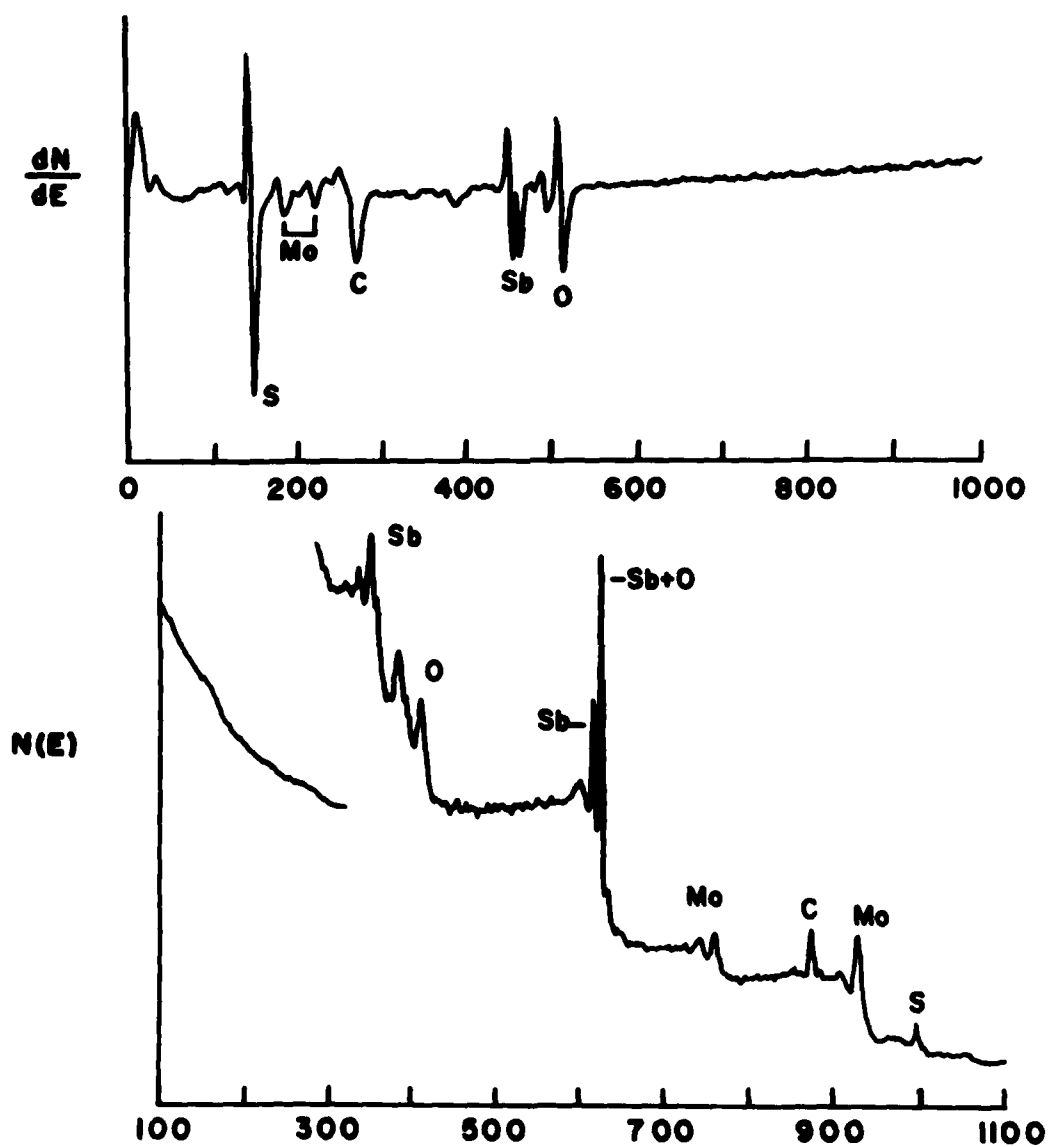


FIGURE 37 - Analysis of co-sputtered MoS_2 and Sb_2O_3 using (a) Auger electron spectroscopy, and (b) X-ray photoelectron spectroscopy.

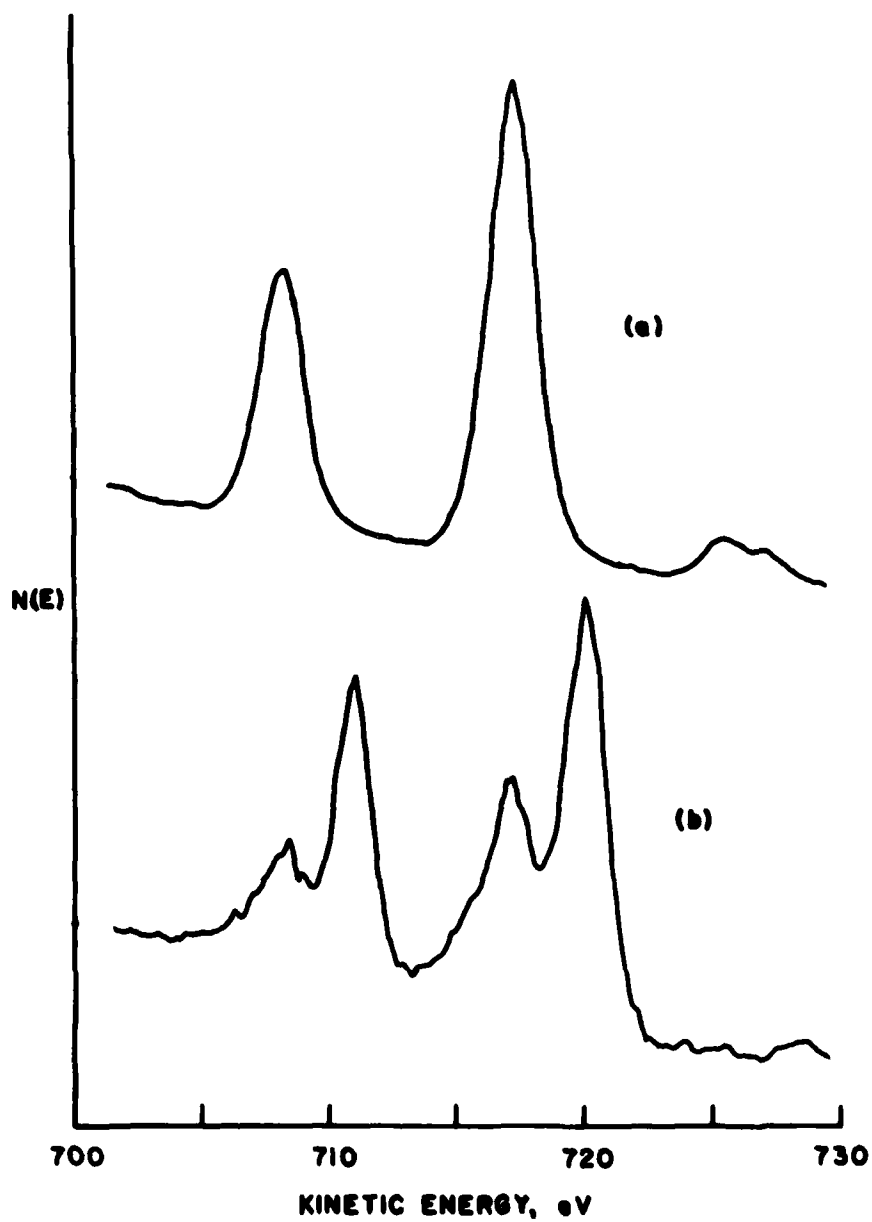


FIGURE 38 - XPS spectra from, (a) $\text{MoS}_2 + \text{Sb}_2\text{O}_3$ burnished film, and (b) partly oxidized InSb. Spectrometer resolution was 1 eV.

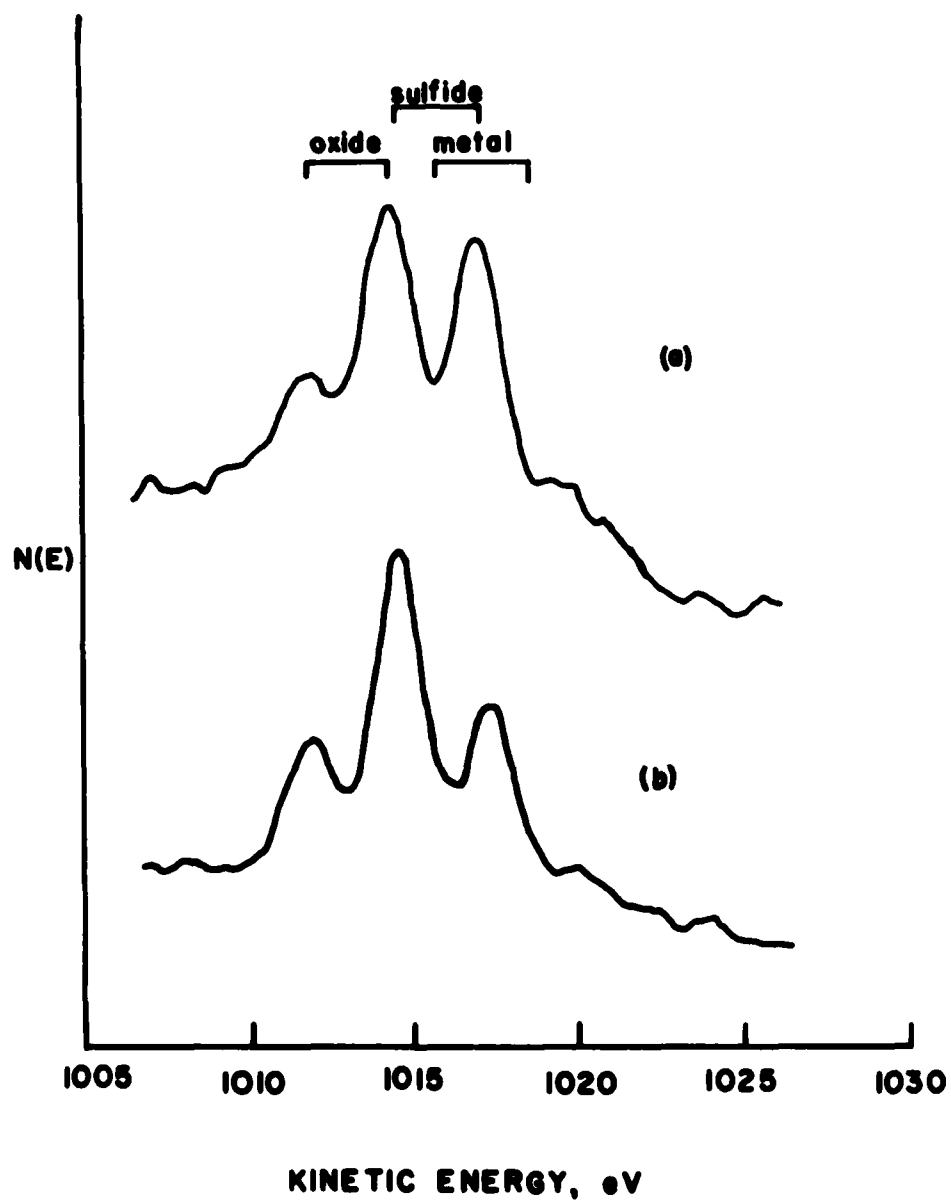


FIGURE 39 - Molybdenum 3d XPS spectra from two partly worn gas bearings, (a) and (b). Spectrometer resolution was 1 eV.

are present on the partly worn bearings. Molybdenum 3d reference spectra were obtained and are shown in Figure 40, (a) being from (air) oxidized molybdenum, (b) from a burnished molybdenum disulfide film and (c) from clean molybdenum. The positions of these reference spectra are also shown in Figure 39. Identification of the two main chemical states of molybdenum on the bearings is now quite clear, a mixture of molybdenum oxide and molybdenum disulfide. Note that the bearing in Figure 39 (b) is more oxidized than that in Figure 39 (a).

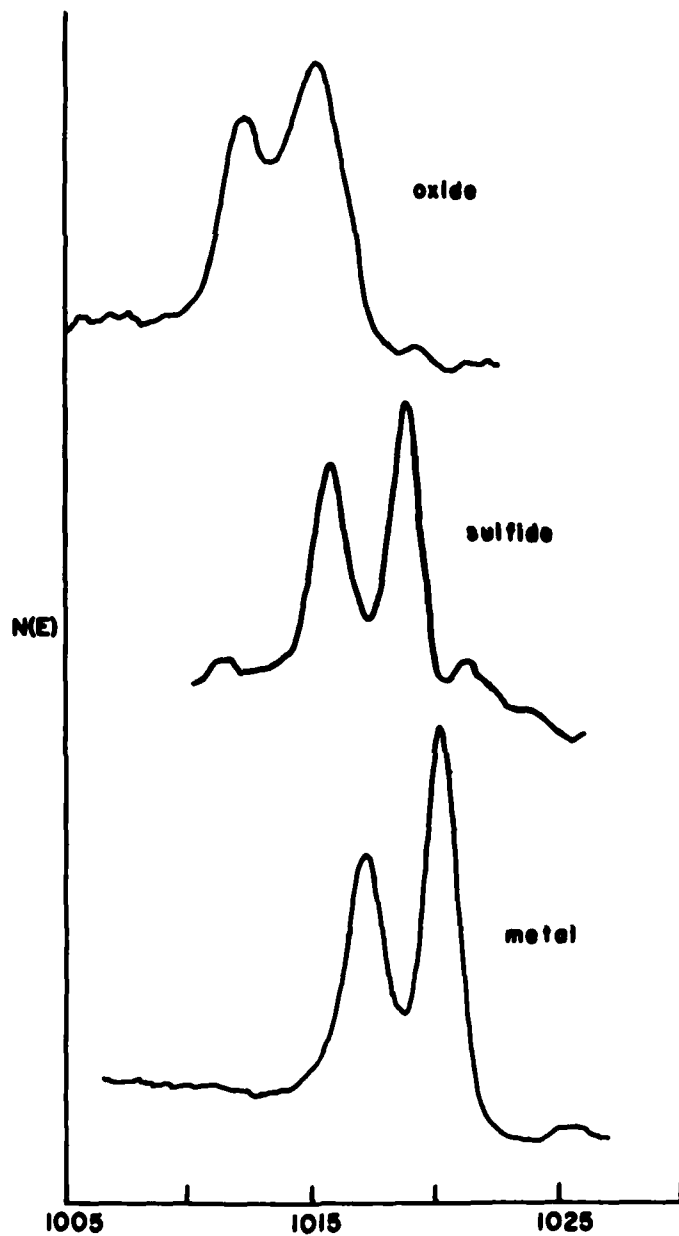


FIGURE 40 - Molybdenum 3d XPS spectra from, (a) air oxidized molybdenum, (b) burnished MoS_2 film, and (c) clean molybdenum. Spectrometer resolution was 1 eV.

SECTION VII

OTHER SURFACE STUDIES

1. ELECTRON BOMBARDMENT OF BORON NITRIDE

A study was undertaken to investigate possible changes in surface composition and chemistry during electron bombardment of boron nitride (BN). Two types of BN were analyzed -isotropic BN and anisotropic BN. BN is used as an insulating material in traveling wave tubes (TWT) and if degradation of BN occurred under electron bombardment it could lead to premature failure of TWT's.

Both AES and XPS measurements were made before and after bombardment. Electron bombardment was carried out with a 30 μ A, 5kV electron beam having a beam diameter of about 1mm. Under such conditions many compounds suffer surface decomposition, but no such decomposition was observed for BN. Reference AES and XPS spectra of boron were also taken and it was quite apparent that if significant decomposition occurred it would have been detected. The level of detectability for a change in surface composition or chemistry of BN is estimated to be about 10%. The only change noted was an increase in the surface carbon concentration with bombardment time, due to electron beam cracking of carbon containing gases in the vacuum chamber on the BN. (The background pressure was about 2×10^{-8} Pa during bombardment.

2. ANALYSIS OF ANGLE OF ATTACK TRANSMITTER

AES analysis of components of an F-4 angle of attack transmitter were made to determine the presence of NbSe₂ lubricant on parts. NbSe₂ was used as a lubricant for the slide wire in the transmitter and it was thought that some NbSe₂ may have reached the bearings in the transmitter.

Analysis of the bearing showed no NbSe_2 lubricant was present. Auger analysis of the slide wire also showed no NbSe_2 was present on the slide wire although significant amounts of Si, Zn, C and O were found. After inert gas sputtering Pt and Rh were detected, indicative of the composition of the slide wire. The contact wire showed Si, Zn, N and Cl before sputtering and Pd, Ag, Cu and Al after sputtering.

3. ANALYSIS OF ANODIZED MERCURY CADMIUM TELLURIDE

Mercury Cadmium Telluride is currently being developed as a wide band IR detector and as such is of considerable interest. A sample of anodized Hg Cd Te was depth profiled using AES, the resulting profile being shown in Figure 41. Several interesting features are apparent. The first is the complete absence of Hg from the oxide layer. The second is that the relative signal intensities of Te and Cd from the surface are nearly the same as those from the bulk, but that they change considerably in the oxide layer, with the cadmium becoming the more intense signal. The dip in the intensity in the tellurium signal at the oxide-bulk interface is probably due to a change in the peak shape due to the change in the chemical environment.

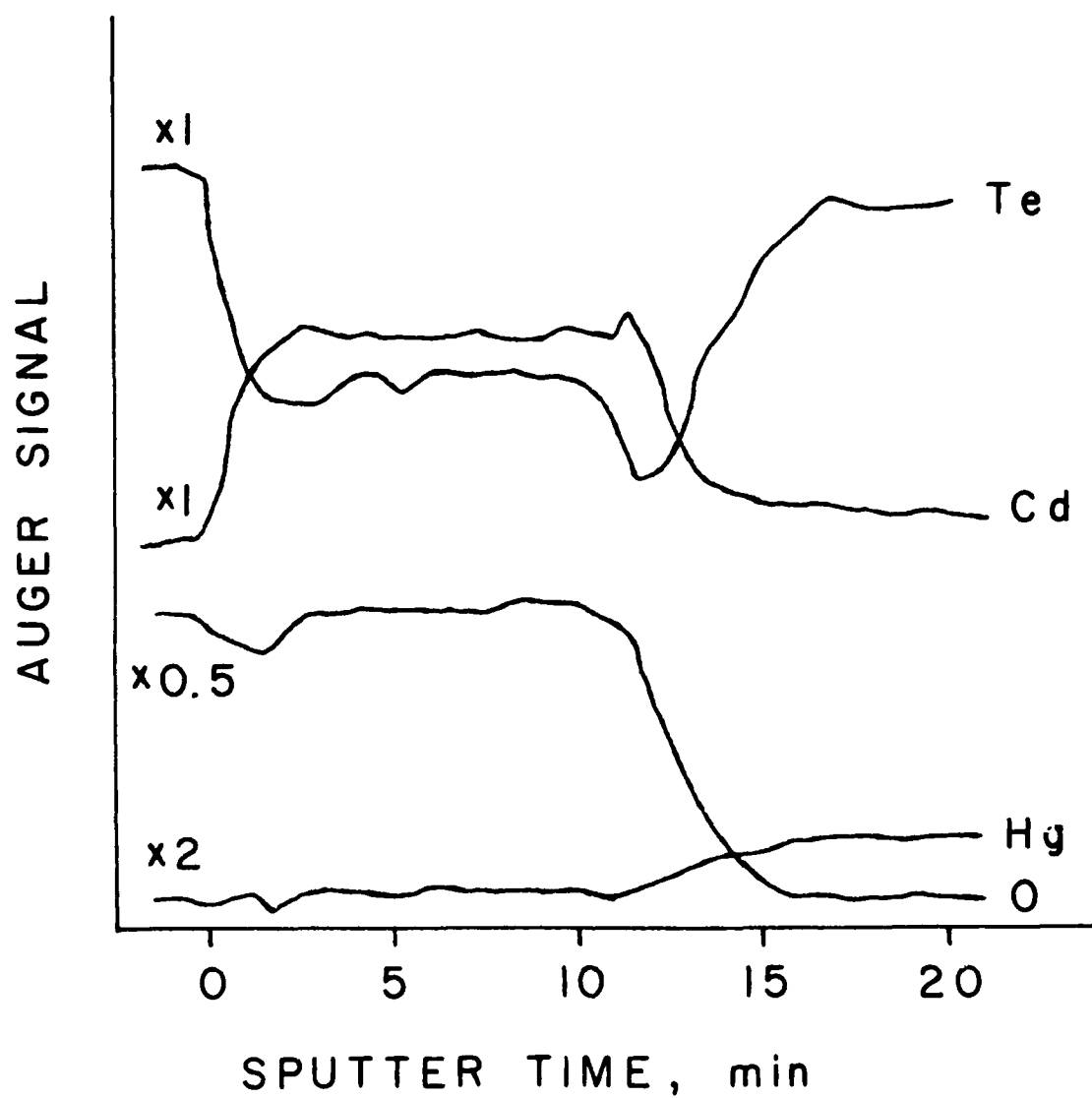


FIGURE 41 - AES depth profile of anodized Hg Cd Te.
Modulation was 6 eV peak-to-peak.

APPENDIX

A Deconvolution Program for XPS Data

```
10=  PROGRAM DECON(INPUT,OUTPUT,TAPE 1=OUTPUT,TAPE 2=INPUT,TAPE 3
20=  1, TAPE 4,TAPE 6)
30=  DIMENSION F(1000),G(1400),H(1000),X(1000),Y(1000),CH(1000)
40=  CHECK=1.0
50=  WRITE 10
60=10  FORMAT(/,*NUMBER OF DATA POINTS...*)
70=  READ*,N
80=  DO 20 I=1,1400
90=  G(I)=0.0
100=20  CONTINUE
110=  READ (3,30) (CH(I),H(I),I=1,N)
120=30  FORMAT (2F13.6)
130=  DO 50 I=1,N
140=  X(I)=H(I)
150=50  CONTINUE
160=  READ (6,40) (G(I),I=351,1050)
170=40  FORMAT (F13.6)
180=  WRITE 60
190=60  FORMAT (/,*WIDTH OF DECONVOLUTION REGION IS 2L+1' ENTER L...*)
200=  READ*,L
210=  IMIN=1+L
220=  IMAX=N-L
230=190  CONTINUE
240=  WRITE 80
250=80  FORMAT(/,* ENTER NUMBER OF APPROXIAMTIONS TO BE MADE...*)
260=  READ*,KMAX
270=  DO 90 K=1,KMAX
280=  DO 310 I=1,N
290=  Y(I)=0.0
300=310  CONTINUE
310=  DO 100 I=IMIN, IMAX
320=  JMIN=I-L
```

```

330=    JMAX=I+L
340=    DO 110 J=JMIN,JMAX
350=    ISUB=700+J-I
360=    Y(I)=X(J)*G(ISUB)+Y(I)
370=110 CONTINUE
380=100 CONTINUE
390=    DO 320 I=IMIN,IMAX
400=    IF (Y(I).LT.0.0) CHECK=10.0
410=    IF (CHECK-10.0) 320,330
420=330 WRITE (1,340) I
430=340 FORMAT (/,1X,*Y(I) LESS THAN 0*, 5X,I3)
440=    GO TO 180
450=320 CONTINUE
460=349 FORMAT (5X,F13.6,5X,F13.6)
470=    DO 120 I=IMIN,IMAX
480=    X(I)=X(I)*H(I)/Y(I)
490=120 CONTINUE
500=90  CONTINUE
510=    WRITE 170
520=170 FORMAT(/,*TOTAL NO. OF APPROX. TO BE MADE...*)
530=    READ*,MAX
540=    IF (MAX-KMAX) 190,180
550=180 CONTINUE
560=    WRITE (4,230) CH(I),X(I),I=IMIN, IMAX)
570=230 FORMAT (2F13.6)
580=    NX=IMAX-IMIN+I
590=    WRITE (1,240) NX
600=240 FORMAT (1X,I3,* DATA POINTS TO BE PLOTTED ARE ON TAPE 4*)
610=350 END

```

REFERENCES

1. J. H. Scofield, J. Electron Spectrosc. Relat. Phenom., Vol. 8, pp. 129 (1976).
2. K. A. G. MacNeil and R. N. Dixon, J. Electron Spectrosc. Relat. Phenom., Vol. 11, pp. 315 (1977).
3. N. Beathan and A. F. Orchard, J. Electron Spectrosc. Relat. Phenom., Vol. 9, pp. 129 (1977).

EN

DATE
FILME

6-8

DTIC